JOURNAL OF GEOPHYSICAL RESEARCH, VOL. 105, NO. E9, PAGES 22,455–22,486, SEPTEMBER 25, 2000

North polar region of Mars: Topography of circumpolar deposits from Mars Orbiter Laser Altimeter (MOLA) data and evidence for asymmetric retreat of the polar cap

Kathryn E. Fishbaugh and James W. Head III

Department of Geological Sciences, Brown University, Providence, Rhode Island

Abstract. We have used high-resolution Mars Orbiter Laser Altimeter (MOLA) data to analyze the topography, morphology, stratigraphy, and geologic history of the Martian north circumpolar deposits. The present polar deposits are offset about toward 0°W from the rotational pole. An arc of irregular topography, concentric to Olympia Planitia and the cap, consists of polar material remnants, depressions which we interpret to be kettles, frost-covered and residual ice-filled craters, and frost patches. Olympia Planitia, originally thought to be a flat, sand-covered plain, is characterized by a convex-upward topography, contiguous with the polar cap. We interpret Olympia Planitia to represent a now dune-covered extension of the polar materials. Together, Olympia Planitia and the outlying deposits delineate a former extent of the polar cap. Topographic data have clarified relationships among the circumpolar deposits. Contributors to these deposits include local volcanics, fluvial and aqueous sediments (from outflow channels and a possible standing body of water), pyroclastic ash, sublimation lag from the Olympia Lobe, and eolian-reworked materials. Significant events in the history of the region include (1) formation of the northern lowlands; (2) emplacement of volcanic plains, fluvial and aqueous sedimentation, and subsequent desiccation, forming polygonal patterns which in part underlie the present polar layered deposits; (3) formation of the polar cap, composed primarily of layered deposits; (4) asymmetric retreat of the Olympia Lobe, resulting in sublimation lag deposits, polar remnants, and kettles; and (5) continued collection and reworking of sediments by eolian processes. The cause of the asymmetrical retreat of the Olympia Lobe is unknown.

1. Introduction

1.1. North Polar Region

The north polar region of Mars has had a complex geologic history. It resides in the lowest point of a basin that extends over nearly the entire Northern Hemisphere [*Head et al.*, 1998; *Zuber et al.*, 1998a]. Thus this region is an ideal location for the deposition of outflow channel fluids and sediments [*Baker et al.*, 1992] and formation of possible large standing bodies of water in the history of Mars [*Parker et al.*, 1989, 1993; *Clifford and Parker*, 1999]. Volcanic material from the Tharsis region, Alba Patera in particular, extends into the north polar region [*Dial*, 1984; *Tanaka and Scott*, 1987; *Jager and Head*, 1999]. The largest ergs on Mars reside within the circumpolar deposits [*Dial*, 1984; *Tanaka and Scott*, 1987; *Greeley et al.*, 1992]. The main cap contains the largest known reservoir of water on the planet [*Zuber et al.*, 1998a; *Smith et al.*, 1998] and consists of a complex system of layered deposits of ice and possibly dust and sand and deep troughs [*Thomas et al.*, 1992; *Howard*, 1998; *Fisher*, 1993]. *Dial* [1984] and *Tanaka and Scott* [1987] have used Mariner 9 and medium- and high-resolution Viking images to map the north polar region of Mars. The geologic units record a diverse history, with variable amounts of mantling, densities, and states of degradation of craters. Polygonal terrain also lies in the vicinity of the base of the cap [*Lucchitta et al.*, 1986]. While it has been postulated that the polar cap and its mapped patches of outlying residual ice remnants may be a major source for the north polar erg [*Dial*, 1984; *Tanaka and Scott*, 1987], the composition of the layered deposits within the polar cap and the thickness of the layers are not known to sufficient accuracy to substantiate this conclusion [*Thomas et al.*, 1992].

Until the acquisition of high-resolution topographic data from the Mars Orbiter Laser Altimeter (MOLA) several factors concerning the mapped geologic units and complex geological processes have been difficult to constrain. These include the following: (1) the topography of the region as a whole and of the individual geologic units, (2) the stratigraphic relationships of the geologic units and the source of the circumpolar deposits, (3) the topographic nature of the outlying polar residual ice (or frost) remnants mapped by *Dial* [1984] and *Tanaka and Scott* [1987], and (4) the possibility that the cap may once have been larger. The MOLA on the Mars Global Surveyor has provided the high-resolution altimetry necessary for analysis of these issues, and, owing to its polar orbit, MOLA provides extensive coverage of the north polar region.

1.2. MOLA Instrument

MOLA measures the distance between the spacecraft and the surface of Mars with a vertical accuracy of 5 m on a local scale and 30 m on a global scale and with a horizontal resolution of 160 m [*Smith et al.*, 1998; *Zuber et al.*, 1998a]. From MOLA data one can obtain point-to-point and regional slopes, topographic profiles, gridded topographic maps, surface roughness, and surface reflectivity. MOLA has revealed several signifi-

Paper number 1999JE001230.
0148-0227/00/1999JE001230$09.00

cant characteristics of the Northern Hemisphere of Mars, including (1) a smooth surface sloping from the planetary dichotomy boundary down toward the north polar cap [*Smith et al.*, 1998], (2) detailed topography of the polar cap and polar layered terrain [*Zuber et al.*, 1998a], and (3) the topography and roughness of individual features and units within the lowlands [*Ahronson et al.*, 1998; *Head et al.* 1998; *Kreslavsky and Head*, 1999].

1.3. Goals of This Study

The goals of this study were to use MOLA data to address some of the major outstanding questions about the nature of the deposits and sediments surrounding the polar cap [*Soderblom et al.*, 1973a, 1973b; *Squyres*, 1979; *Thomas et al.*, 1992] and their relationship to the cap and the history of the northern lowlands [*Tanaka et al.*, 1992]. To this end, we have used MOLA data to assess (1) the overall topography of deposits surrounding the polar cap (from ~65° to 85°N), (2) the detailed local topography of individual geologic units and unit contacts appearing on the geologic maps of the north polar region [*Dial*, 1984; *Tanaka and Scott*, 1987], (3) the stratigraphy of the mapped units, (4) the origin of sediments surrounding the cap, (5) the nature of the mapped polar material outliers, and (6) the implications for the former larger extent of the main cap. For the purposes of this study, we have used a 1/4° grid of MOLA data covering the region from 75° to 90° N to create a topographic map and perspective views of the north polar region over which the geologic map is draped. We have also analyzed topographic profiles extending fully around the cap and from 65°N to 85°N. By overlaying these MOLA tracks on the geologic map, the locations of significant topographic features as well as geologic unit contacts were noted. Each profile was color-coded according to the geologic units traversed and stacked vertically for comparison.

We use the following definitions: polar deposits, in general, consist of polar layered terrain and polar residual ice deposits, the latter being the perennial ice deposits [*Dial*, 1984; *Tanaka and Scott*, 1987]. These are distinguished from polar seasonal frosts and deposits [*Thomas et al.*, 1992; *Cantor et al.*, 1998; *Forget*, 1998]. The seasonal frost leaves ice-rich material at very high latitudes after the frost has retreated, thus adding to the residual ice cap [*Clifford et al.*, 2000]. Circumpolar deposits consist of the geologic units surrounding and possibly underlying the main cap and deposits more specifically characterized by a range of surface dune types [*Dial*, 1984; *Tanaka and Scott*, 1987].

2. Background

2.1. Age of the Polar Deposits and Geologic History

Although the north polar deposits are some of the relatively youngest units on Mars, little is known about their absolute age, including their time of formation and deposition and their history [e.g., *Thomas et al.*, 1992; *Plaut et al.*, 1988]. Estimates of the age of the Martian polar deposits range from a minimum of <100 Kyr [*Herkenhoff et al.*, 1997; *Clifford et al.*, 2000] for the presently exposed surface deposits (using the observation that, according to *Cutts et al.* [1976], no fresh craters have been found on the dunes), to a maximum of >100 Myr for the presently exposed south polar deposits [*Plaut et al.*, 1988] (using an estimation of the sedimentation rate and a steady-state cratering model). *Herkenhoff and Plaut* [2000] have since revised this latter estimate to 7 –15 Myr. This large uncertainty in the ages, mostly due to differences in crater-counting statistics and in calculation of sedimentation rates [*Thomas et al.*, 1992], makes it difficult to interpret the interaction of the polar and circumpolar deposits from crater counts alone.

According to *Dial* [1984] (Plate 1 and Figure 1), the geologic history of the region is highlighted by the early formation of volcanic plains in Hesperian and early Amazonian times and by interaction with polar volatiles to produce palagonite and other physical weathering products to form the mantled plains materials. Eolian processes then removed and redistributed this material during middle Amazonian time. The presently observed polar materials (Apr and Apl) are thought to have been emplaced at about the same time as the younger mantled plains, although the time of formation of the earliest residual cap is unknown. The extensive polar dune fields cover many of the older units near the residual cap, and the process of their formation is active today.

Tanaka and Scott [1987] (Plate 2 and Figure 2) have proposed that the Vastitas Borealis Formation, which covers much of the northern lowlands, was emplaced during the middle to late Hesperian and consists of alluvial and eolian sediments and lava flows. The polar layered terrain was deposited during the early Amazonian, possibly related to fluvial processes. The presence of layered terrain outliers is interpreted to indicate past and possibly current erosion of this terrain. Outliers of residual polar material are mostly stable over small timescales but may change shape and location with long-term changes in climate. The extensive circumpolar ergs are thought to represent a large sand supply that has collected in a topographic low over some time. These dunes may have originated from erosion of the layered deposits.

2.2. Sources of Circumpolar Deposits

We summarize several candidate sources for deposits in the northern lowlands, including circumpolar deposits. These sources could exist in some combination:

1. Volcanic ash from Alba Patera, Elysium Mons, Olympus Mons, and Amazonis Planitia could be transported northward and redistributed over a broad region in the north polar area; some of this ash could have been contributed throughout the history of the northern lowlands and could reside in the residual ice cap [*Dial*, 1984].

2. Other sources of fines could be comminution by impacts and mass wasting of highland material along the highland-lowland boundary in areas of knobby and fretted terrain.

3. Lava flows from Alba Patera could enter the distal portions of the north polar region and form alteration products owing to interaction with water.

4. Sublimation of the polar cap could allow deposition into Olympia Planitia of the dark dust layers within [*Thomas et al.*, 1992; *Thomas and Weitz*, 1989]. The close proximity of the circumpolar deposits to the polar deposits and the evidence cited above for the former greater lateral extent of the polar deposits strongly suggest that the modification and erosion of previous polar deposits was a significant source for sediments presently observed in the circumpolar mantling deposits. According to *Thomas and Weitz* [1989], dune-forming sediments exist within the southern and northern layered deposits and have albedos and colors similar to dunes elsewhere on Mars.

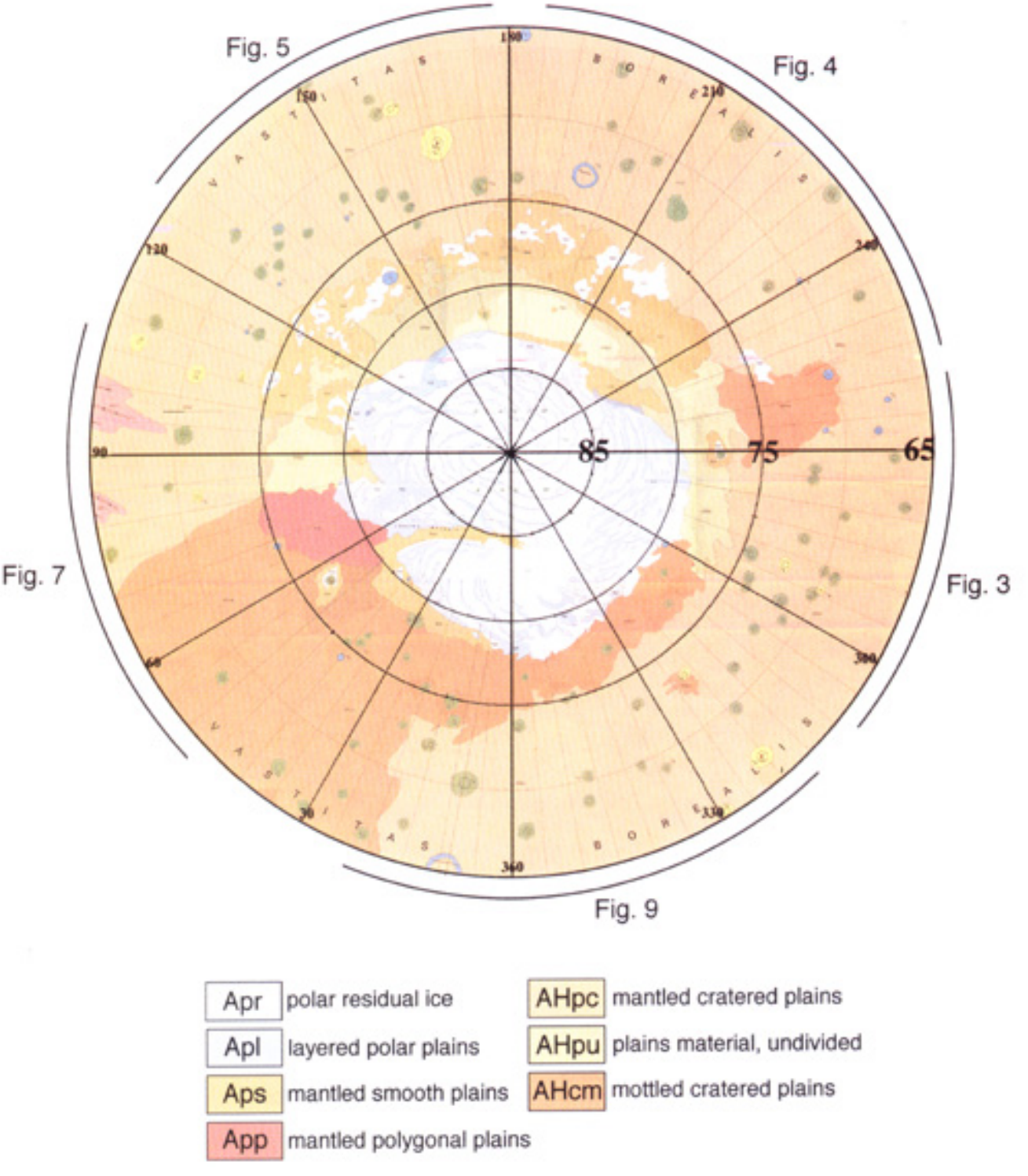

Plate 1. Geologic map of the Mare Boreum region of Mars [*Dial,* 1984]. Scale is 1:5M. The MOLA orbits discussed in this paper have been superposed on the map so that the profiles in Figures 1-3, 5 and 7 can be located on the map.

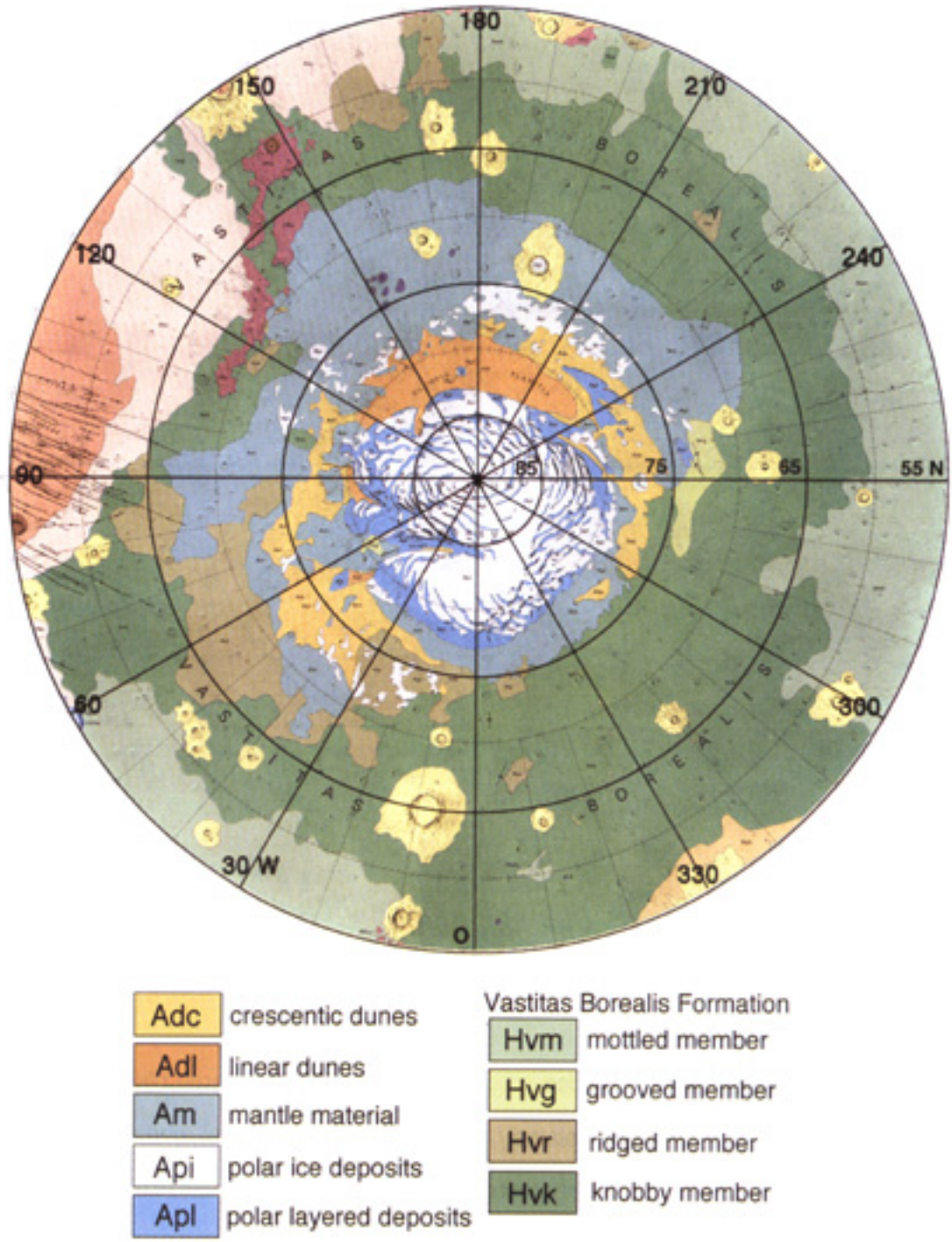

Plate 2. North pole portion of *Tanaka and Scott*'s [1987] geologic map of the polar regions of Mars.

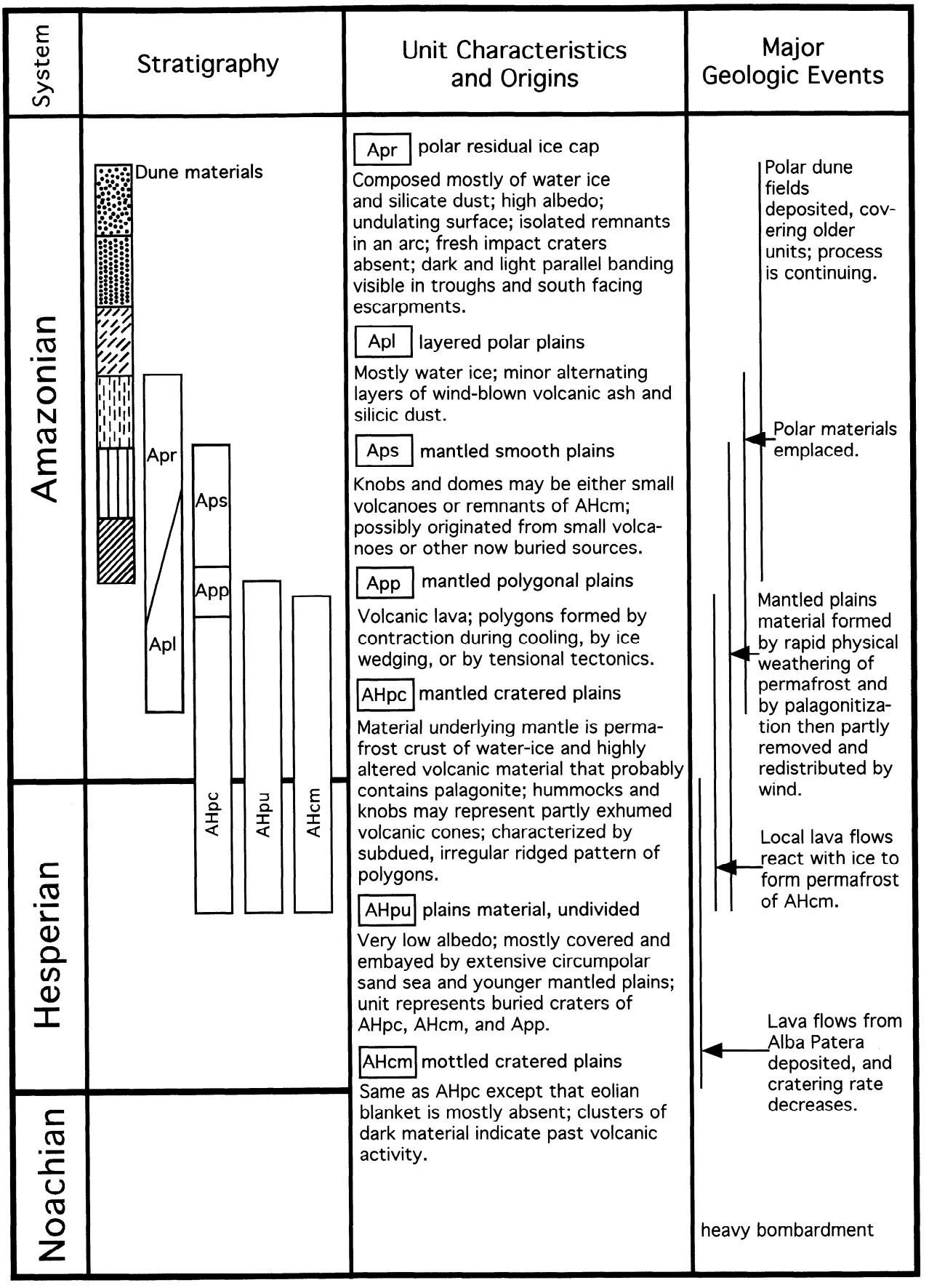

Figure 1. Stratigraphic column modified from *Dial* [1984].

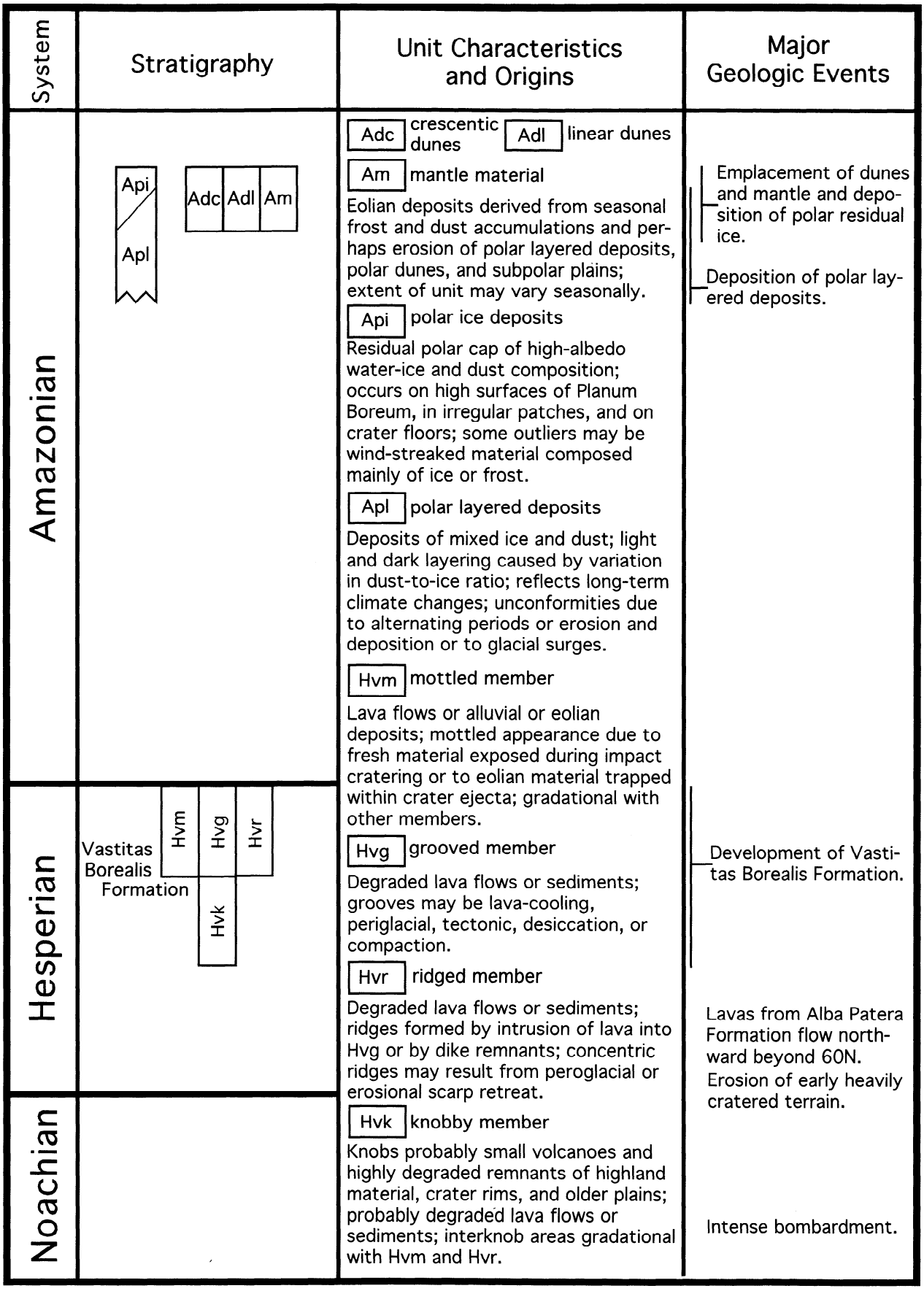

Figure 2. Stratigraphic column modified from *Tanaka and Scott* [1987].

5. Global dust storms could bring sand and dust into the region [*Khan et al.*, 1992].

6. Fluvial and related lacustrine/marine processes may have deposited material in one or a combination of four ways: (1) deposition of course-grained material in a slurry of water and sediment from outflow channels, (2) settling of fine-grained material within a standing body of water, (3) deposition via turbidity currents caused by inflow of water from outflow channels into a standing body of water which would tend to leave sediments in the lowest topographic regions, and (4) deposition of evaporites (due to the presence of S and Cl salt compounds in the Martian soil [*Banin et al.*, 1992]). Abundant evidence has been cited indicating that the northern lowlands were the site of deposition of water and sediment from outflow channels [e.g., *Baker et al.*, 1992; *Carr*, 1996] during the late Hesperian and Amazonian [*Tanaka et al.*, 1992]. Estimates of the degree of flooding of the northern lowlands ranges from the scale of lakes and seas [e.g., *Scott et al.*, 1995] up to ocean-scale events flooding virtually all of the northern lowlands [e.g., *Parker et al.*, 1989, 1993; *Gulick and Baker*, 1989; *Baker et al.*, 1991; *Clifford and Parker*, 1999]. Analysis of MOLA data to test predictions of models of fluvial processes in terms of detailed basin topography, contact positions, surface smoothness, volumes, and locations of related features (such as polygonal ground) provides results that are generally consistent with the presence of large bodies of water and associated sediments in the northern lowlands in relatively recent history [e.g., *Head et al.*, 1999a, 1999b]. In addition, the presence of the lowest parts of the North Polar Basin [*Head et al.*, 1999a, 1999b] adjacent to and surrounding the north pole provides a focal point for the deposition of these sediments. The general smoothness and similar roughness values of the subunits of the Vastitas Borealis Formation as compared to the global average at all wavelengths is consistent with sedimentation [*Kreslavsky and Head*, 1999]. Depending on the timing of the deposition of water and sediment as well as on such variables as humidity of the atmosphere, air temperature, and thickness of mantling deposits [*Clifford and Parker*, 2000], buried frozen bodies of water may still exist in the northern plains. Groundwater can also be added to the cryosphere from below by thermal vapor diffusion, seismic pumping, and hydrothermal circulation [*Clifford*, 1993]. In addition, basal melting beneath the polar caps can add groundwater from above [*Clifford*, 1987].

7. Eolian processes are likely to have reworked any of these original deposits.

2.3. Geologic Mapping

2.3.1. *Dial* [1984] map. *Dial* [1984] has mapped the north polar region of Mars (Plate 1) at 1:5M scale, using low-resolution (100-800 m/pixel) Mariner 9 and medium- (100-180 m/pixel) and high-resolution (40-60 m/pixel) Viking 2 Orbiter images taken during the spring and summer, when the seasonal frost cap is at its smallest extent.

According to *Dial* [1984], the mottled cratered plains (AHcm), the oldest of the units and concentrated between 350° and 70°W longitude, are not mantled. Ice and volcanic material form a permafrost crust 3 km thick at the pole in this region. Evidence for ancient volcanic activity can be seen in Viking images of the AHcm in the form of dark ring clusters, irregular clusters of dark material, and dark ridges similar to terrestrial dikes. Beneath this permafrost layer lies liquid and frozen water. The mantled cratered plains (AHpc), largely covering the circumpolar area from 65° to 75°N, are the same as the mottled cratered plains (AHcm), but with a slowly and constantly deposited mantle. The undivided plains (AHpu), mostly covered and embayed by the circumpolar erg, may include mantled and mottled cratered plains (AHcm) and mantled polygonal plains (App) buried by dunes but are presently visible only by the rims of buried craters. The mottled crater plains underlie the mantled polygonal plains (App), which *Dial* [1984] suggests may have been created tectonically, by contraction of lava during cooling or by ice wedging. Much of the mantle in this unit may have been removed by the outflow of meltwater which may have carved Chasma Boreale [*Clifford*, 1987; *Benito et al.*, 1997; *Fishbaugh and Head*, The morphology of Chasma Boreale, Mars using MOLA data: Investigating formation by melting, 2000 (hereafter referred to as manuscript in preparation, 2000)]. The mantled smooth plains (Aps), flat at medium resolution and thought to be mantled volcanics, have been described as being young and having a gradational contact with the mantled and mottled cratered plains (AHcm) and the mantled polygonal plains (App).

The polar deposits, consisting of the polar layered deposits (Apl) and the polar residual ice deposits (Apr), are the youngest units. The layered deposits consist of alternating layers of ice and dust, the mechanism of formation of which is not specifically known but may be due to seasonal and/or obliquity variations [*Thomas et al.*, 1992; *Toon et al.*, 1980]. The main cap consists of Apl and Apr and is characterized by a spiraling pattern of troughs which expose the layered materials and could be migrating poleward [*Howard et al.*, 1982; *Fisher*, 1993]

The Apr unit can be found as part of the main cap and as residual polar material outliers in an arc centered at 180°W and extending from ~75° to 80°N and ~95° to 255°W. One of these outliers has dark features associated with eolian processes [*Dial*, 1984]. The temperature of the outliers is lower than the surrounding terrain but higher than the cap [*Kieffer et al.*, 1976, *Kieffer et al.*, 1977; *Paige et al.*, 1994]. This temperature difference is proposed by *Dial* [1984] to mean that the outliers are less thick than the cap and are able to be more easily eroded by eolian processes. *Dial* [1984] also postulates that the main residual cap contains some volcanic ash and some dust and thus that the outliers of the cap could have been a source for the ergs. *Thomas et al.* [1992] propose that these outliers are remnants of the seasonal CO_2 frost cap that have persisted owing to shading by local topographic prominences or owing to eolian redistribution. *Thomas et al.* [1992] note that remnants of the seasonal frost cap remain within impact craters and other topographic features and that these may be thicker frost deposits which have resulted from shading by topography and from redistribution of material by eolian processes. Thus the question arises as to whether these outliers simply represent seasonal remnants in thermally favorable local environments or whether they might represent longer-term residual polar material remnants.

2.3.2. *Tanaka and Scott* [1987] map. Somewhat different units were introduced as part of the 1:15M-scale global geologic mapping effort [*Tanaka and Scott*, 1987] (Plate 2). The authors map much of the northern lowlands below ~70°N as subdivisions of the Vastitas Borealis Formation (Hv), and the subunits are generally interpreted to be volcanic units modified to varying degrees. Younger Amazonian units dominate poleward between about 75° and 85°N, including extensive

mantle material (Am) interpreted to be of eolian origin and to overlie Hv. Linear dune material (Adl) is thought to represent sand accumulation in local topographic lows [*United States Geological Survey (USGS)*, 1991] (most prominently Olympia Planitia) and to indicate a large sand supply deposited in a topographic basin over a long period of time [*Breed et al.*, 1979]. Crescentic dune material (Adc) is interpreted to form where sand supply is less and more transient [*Breed et al.*, 1979]. Polar deposits are interpreted as consisting of residual polar ice (Api) and polar layered deposits (Apl). *Tanaka and Scott* [1987] describe the mapped outliers of Api as wind-streaked, outlying mesas of ice or frost, some of which can be found within crater floors. The authors postulate the outliers to be altered by long-term climatic variations. The center of the cap is displaced ~200 km south (in the 0°W longitude direction) of the axial pole position away from the extensive linear dune and mantle deposits; this displacement is attributed to prevailing wind patterns [*Breed et al.*, 1979].

2.3.3. Map differences. Several differences exist between the *Tanaka and Scott* [1987] and the *Dial* [1984] maps. Those relevant to this study are the following. (1) The polar material outliers are different shapes, and additional ones can be found on the *Tanaka and Scott* [1987] map between 10° and 70°W and 70° and 75°N. (2) *Tanaka and Scott* [1987] have mapped some of the outliers as isolated patches of polar layered terrain at 265°W, 74°N; 235°W, 79°N; and 55°W, 77°N. (3) *Tanaka and Scott* [1987] map the Olympia Planitia region as consisting wholly of Adl without including a section of mantled smooth plains (Aps) between the dunes and the cap. (4) On the *Tanaka and Scott* [1987] map, Chasma Boreale has a small dune unit (Adl) on its floor but is composed mainly of polar layered terrain (Apl). (5) The oldest units on the *Tanaka and Scott* [1987] map are Hesperian in age, while the oldest units on the *Dial* [1984] map are Amazonian-Hesperian in age. (6) The scales and mapped areas are different, the *Tanaka and Scott* [1987] 1:15M map extending from 55° to 90°N and the *Dial* [1984] 1:5M map, extending from 65° to 90°N. In addition, the geologic units mapped on *Tanaka and Scott*'s [1987] map are correlated with the unit definitions from a global mapping effort. Thus the deposits immediately surrounding the pole are more detailed on the latter map. It is for this reason that the stacked profiles and perspective views have been created using *Dial*'s [1984] units.

2.4. Other Maps

Paige et al. [1994] have created thermal and albedo maps of the north polar region using data from Viking Thermal Mapper. The observations were made early in the Martian summer, when temperatures are at a maximum and the polar residual ice cap is exposed. The best fit thermal inertia and albedo maps show that different morphological features have different thermal inertia. These maps can be used to distinguish between frost/ice and sediment and to compare/contrast the thermal conductivity of different sediments in order to determine whether or not different features are genetically related [*Paige et al.*, 1994].

Kreslavsky and Head [1999] have mapped kilometer-scale slopes in the north polar region using MOLA data. Median slopes have been calculated as point-to-point slopes (0.4 km between points) and for six different baselines: 0.8, 1.6, 3.2, 6.4, 12.8, and 25.6 km. The resolution of the surface roughness map is ~15 km for latitudes between 55° and 87°N. The roughness map shows varying characteristics between different surface features which, like thermal inertia data, can be used to determine similar genetic and postformation modification relationships between the various geologic units.

We now use MOLA data, together with the geologic [*Dial*, 1984; *Tanaka and Scott*, 1987], thermal and albedo [*Paige et al.*, 1994], and slope [*Kreslavsky and Head*, 1999] maps, to assess and better constrain (1) the topographic characteristics of the region as a whole and of each geologic unit and unit contact, (2) the stratigraphic relationships between units, and (3) the source of the circumpolar deposits.

3. Observations and Discussion

We have used MOLA topographic profiles to produce three products: (1) a topographic map of the northern high latitudes showing the nature of the topography in the circumpolar region (Plate 3), (2) perspective views of the geologic map superposed on the topographic data (Plate 4), and (3) topographic profiles color-coded according to geologic unit [*Dial*, 1984] and stacked for comparison (Figures. 3-5, 7, and 9). We first describe the general topography, then systematically describe the relationships of topography and geologic units [*Dial*, 1984; *Tanaka and Scott*, 1987], then the nature of the mapped polar material outliers using MOLA data and the 1.75 km resolution Viking mosaic, and finally we describe a geologic history of the region.

3.1. General Topography and Perspective Views

Analysis of the general topographic map and geologic map [*Dial*, 1984] perspective views shows that the terrain surrounding the cap slopes downward toward the cap [*Smith et al.*, 1998; *Zuber et al.*, 1998a] (Plates 3 and 4). Although the general trend is down from lower latitudes toward the north polar cap, MOLA topography shows that the circumpolar region has important variations related to regional structure. The North Polar Basin is not simply a circular basin centered on the cap (Plates 3 and 4c). Alba Patera represents a major incursion of topography from the direction of 90°-150°W (Plate 3). If this topography is constructional, it means that significant products from this eruptive center contributed to North Polar Basin evolution. The North Polar Basin itself is low and elongated toward the 0°-60°W direction, extending toward Chryse Planitia, the source region of six of the major outflow channels [*Baker et al.*, 1992] (Plates 3 and 4c). These data, together with a reanalysis of the Chryse Basin topography [*Ivanov and Head*, 1999], indicate that major Chryse outflow channels would empty directly into the lowest part of the North Polar Basin. In the 180°-270°W direction (Plate 3), the arcuate rim of the adjacent Utopia Basin can be seen, as can the narrow depression (210°-240°W) connecting the Utopia and North Polar Basins [*Thomson and Head*, 1999]. The most prominent topographic perturbation within the North Polar Basin is the presence of the north polar cap itself.

There is a first-order correlation of the major topographic components of the northern lowlands and the geologic units of *Dial* [1984]. First, the Hesperian-Amazonian mantled cratered plains (AHpc) extend from ~75°W clockwise to ~10°W (Plate 4), almost completely around the upper slopes of the parts of the northern lowlands illustrated in Plate 3.

Second, the mottled cratered plains (AHcm) are concentrated primarily in the lowest parts of the North Polar Basin (20°-

75°W) (Plate 4c). The polygonal plains (App) lie within the basin as well, near the mouth of Chasma Boreale. The location and flat, low-lying topography make the basin a possible area of sediment deposition from outflow channels [*Baker et al.*, 1992] and a possible former standing body of water [*Parker et al.*, 1993]. Thermal inertia maps show that the basin has a low albedo with high thermal inertia at 60°N but intermediate thermal inertia at 75°N. This lower albedo may be due to the presence of fluvial and/or oceanic sediments, with varying grain sizes and thicknesses of sediment cover producing different thermal inertia values. The edge of the cap is most steeply sloped (~1°-5°) near the basin and between 310° and 360°W, where the mantled polygonal plains (App) and mottled cratered plains (AHcm) lie at the cap base (Plate 4c). Here the albedo is also low, again possibly owing to the presence of fluvial and/or oceanic sediments. Thus the mantled polygonal plains (App) and mottled cratered plains (AHcm) may underlie some, if not all, of the cap.

Third, in the region of Olympia Planitia (120°-220°W), previously thought to be a flat plain, there is an arcuate prominence and a convex topographic slope tilting toward 180°W from the north polar cap and extending south for several hundred kilometers in the region of a significant occurrence of undivided plains (AHpu) (Plates 4a and 4b).

Fourth, south of this region, but within the same longitude band, there is a distinct arcuate topographic low that is generally circumferential to the Olympia Planitia region and extends to ~70°N (Plates 3 and 4a) [e.g. *Johnson et al.*, 2000]. The area has some of the roughest topography of the mapped area [*Kreslavsky and Head*, 1999], containing a series of large, irregular depressions and several craterform structures. In this region, *Dial* [1984] and *Tanaka and Scott* [1987] have mapped detached polar material and a very high concentration of the smooth plains (Aps). When Olympia Planitia is included in the overall distribution of polar topography, along with the arc of polar material outliers, the general symmetry of the topography of Planum Boreum around the rotational pole position is restored. This suggests that the residual polar deposits may once have been larger, extending south to the arc of polar material outliers.

Last, the present topographic high point of the residual cap is close to the rotational pole (Plates 3a and 4b) [*Zuber et al.*, 1998a]. The cap is ~3 km thick and has an estimated total volume of ~1.2 - 1.7x10^6 km^3 [*Zuber et al.*, 1998a]. The cap consists of polar residual ice (Apr) and polar layered deposits (Apl) and has spiraling troughs. The high topography of the polar layered materials in Plate 4 implies that the cap may consist mostly of polar layered material with a thinner layer of purer water-ice on the surface. Thermal inertia data support this conclusion. According to *Paige et al.* [1994], the polar layered materials have high thermal inertia and are thus composed of either sedimentary material bonded by water-ice or of dirty water-ice. This interpretation is further substantiated by the observation of water vapor saturation in the atmosphere above these deposits [*Paige et al.*, 1994]. These observations led the authors to the conclusion that the polar layered deposits and polar residual ice can be considered to be the same unit [*Paige et al.*, 1994]. *Clifford et al.* [2000] propose that the current polar residual ice may just be an icy layer in the layered deposits, an unconformity, or a transition between layers in the layered deposits. Parts of the mapped edge of the cap are smooth on a 0.4 km scale [*Kreslavsky and Head*, 1999] and appear to be flat; these regions are occupied in many places by layered terrain and probably represent seasonal frost and moderate-albedo polar layered materials.

The largest of the troughs, Chasma Boreale (Plates 3 and 4c), may have been formed by a separate process such as outflow of glacial meltwater [*Clifford*, 1987; *Benito et al.*, 1997; *Fishbaugh and Head*, 1999, manuscript in preparation, 2000]. A similar origin has been proposed for Chasma Australe in Mars' southern cap [*Anguita et al.*, 1998, 2000]. Mantled smooth plains (Aps) and dunes occupy the floor of Chasma Boreale.

3.2. Detailed Cross Sections

Examination of topographic profiles yields more information about detailed topography of the various geologic units and unit contacts. From these observations we can establish stratigraphic relationships and assess models of geologic history.

Representative stacked profiles illustrating the characteristics of the topography and the relationships among geologic units [*Dial*, 1984] are shown in Figures 3-5, 7, and 9. While Dial's units are shown in the stacked profiles for illustration, the observations can also be extrapolated to the units of *Tanaka and Scott* [1987]. The reported slopes are average slopes for the profiles appearing in the stacked profiles. Starting at ~310°W (orbit 246, Figure 1) and proceeding counterclockwise (east) around the map (Plate 1), the mantled cratered plains (AHpc) slope (~0.03°) gently toward the pole (orbits 246, 210, 229, and 267), analogous to *Tanaka and Scott*'s [1987] knobby (Hvk) and mottled (Hvm) members of the Vastitas Borealis Formation. The undivided and mottled cratered plains (AHpu, AHcm), or mantled plains (Am) and crescentic dunes (Adc) of *Tanaka and Scott* [1987], lie at the base of the polar materials, along a continuation of the mantled cratered plains (AHpc) regional slope (orbits 246, 210, and 267) or in a relatively flatter topographic low at the base of the polar materials (orbit 229). The sloping topography of the mantled cratered plains (AHpc), or Hvk and Hvm, may have provided a background upon which the mottled cratered plains (AHcm) and undivided plains (AHpu), or Am and Adc, were deposited. This section of mottled cratered plains (AHcm) may be of the same origin as the mottled cratered plains (AHcm) within the lowest regions of the North Polar Basin, extending beneath the current polar cap.

In orbit 233 (Figure 4) the regional poleward slope of the mantled cratered plains (AHpc) is interrupted by a topographic rise at about 67°-73°N which is made up in part of a patch of mottled cratered plains (AHcm). This rise is near a crater which has been mapped as a moderately degraded crater [*Dial*, 1984; *Garvin and Frawley*, 1998]. This crater has a diameter of ~35 km; therefore some of this rise may consist of crater ejecta material, and some may represent a break in slope (from relatively flat to ~0.07°) due to the presence of the Utopia Basin rim in this region.

East of this region, the mantled cratered plains (AHpc), or Hvm and Hvk, flatten out, although still sloping gently toward the north, and the undivided and mantled smooth plains (AHpu, Aps), or Am and Adc, occupy an increasingly larger portion of the area adjacent to the polar materials (orbits 233, 218, 237, and 220) (Figure 2). Dunes become evident in the mantled smooth plains (Aps) and undivided plains (AHpu) as high-frequency topography fluctuations. Two populations of mantled smooth plains (Aps) become visible. One lies south-

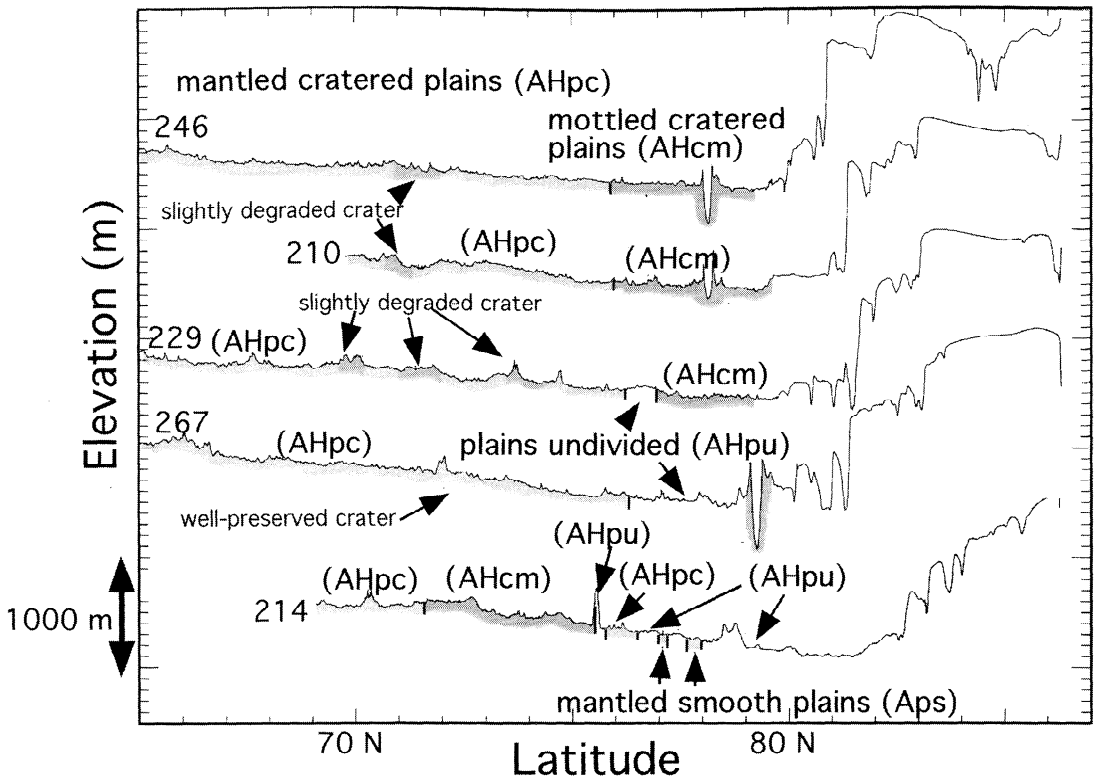

Figure 3. Annotated altimetric profiles (260° -310°; see Plate 1): *Dial*'s [1984] geologic units and mapped craters labeled. No distinction was made between the polar layered terrain and polar residual ice in these annotated profiles. The profiles are labeled by MOLA track number (see Plate 1 for reference). The vertical axis is relative elevation only. Vertical exaggeration is 150x and is the same for each profile. The profiles proceed eastward from the top of the page to the bottom. Illustrated are the gentle slopes of the mantled cratered plains (AHpc) toward the pole and the relatively flatter mottled cratered plains (AHcm) and undivided plains (AHpu) on a continuation of the slope or in a topographic low at the base of the cap.

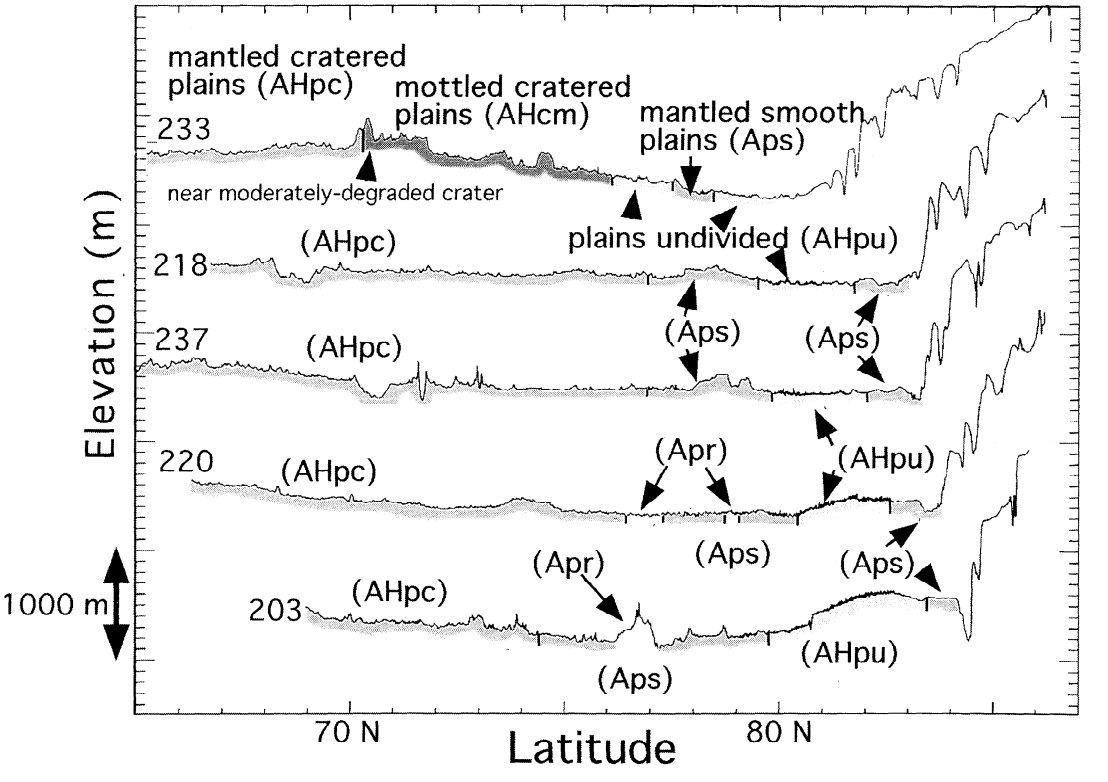

Figure 4. Annotated altimetric profiles (185° -255°; see Plate 1): Gradual flattening of the topography, the location of mantled smooth plains within a flat-lowing region, the appearance of dunes, and the growing positive lobe topography of the undivided plains (AHpu) (Olympia Planitia).

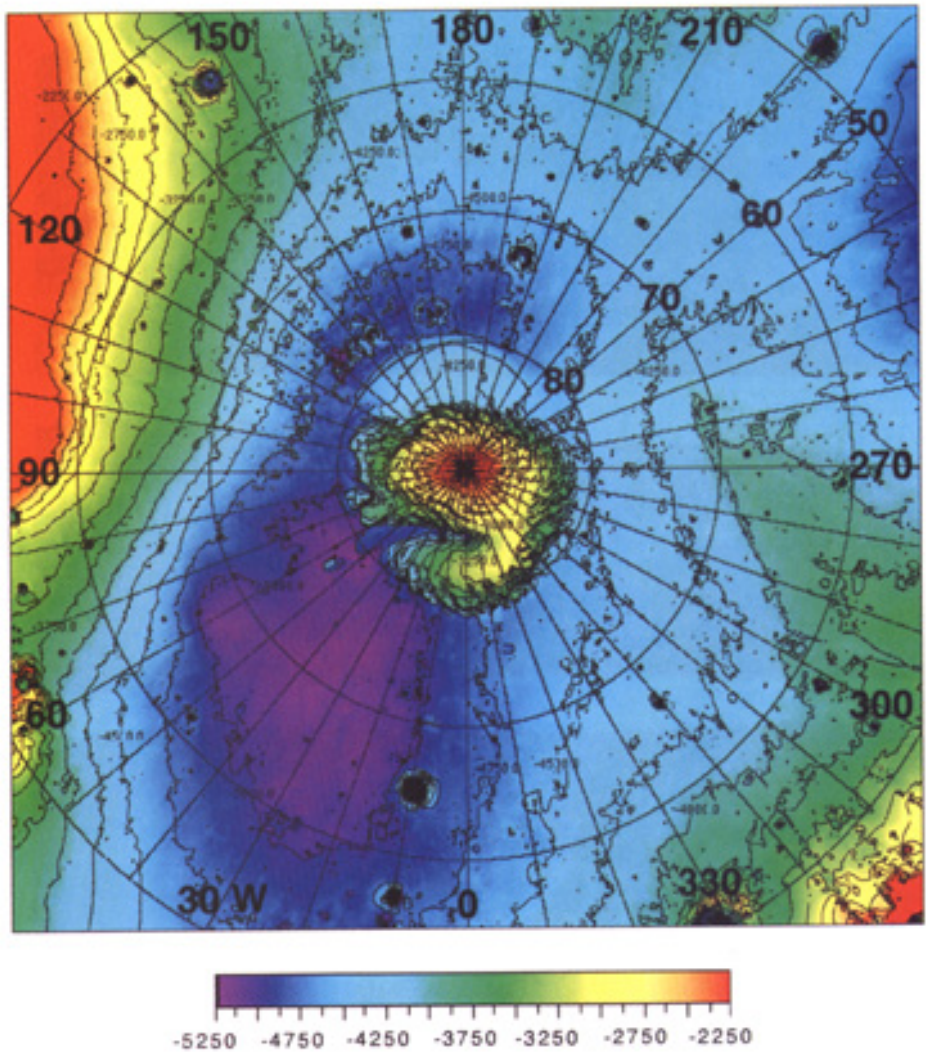

Plate 3. Topographic map of the Martian north polar region. This map shows the lowest parts of the North Polar Basin (0°-90°W), another arc-shaped, low-lying region between 130° and 200°W, and a prominent positive lobe of topography between that low-lying region and the cap. Within the eastern half of the arc-shaped depression lies a rough region containing irregularly shaped topographic prominences and depressions. The terrain surrounding the cap slopes toward the cap so that it lies in a general depression. The cap itself has spiraling troughs and a large reentrant, Chasma Boreale. The topographic high in the top-left corner is part of the flank of Alba Patera, and the topographic low in the top-right corner is part of the Utopia Basin.

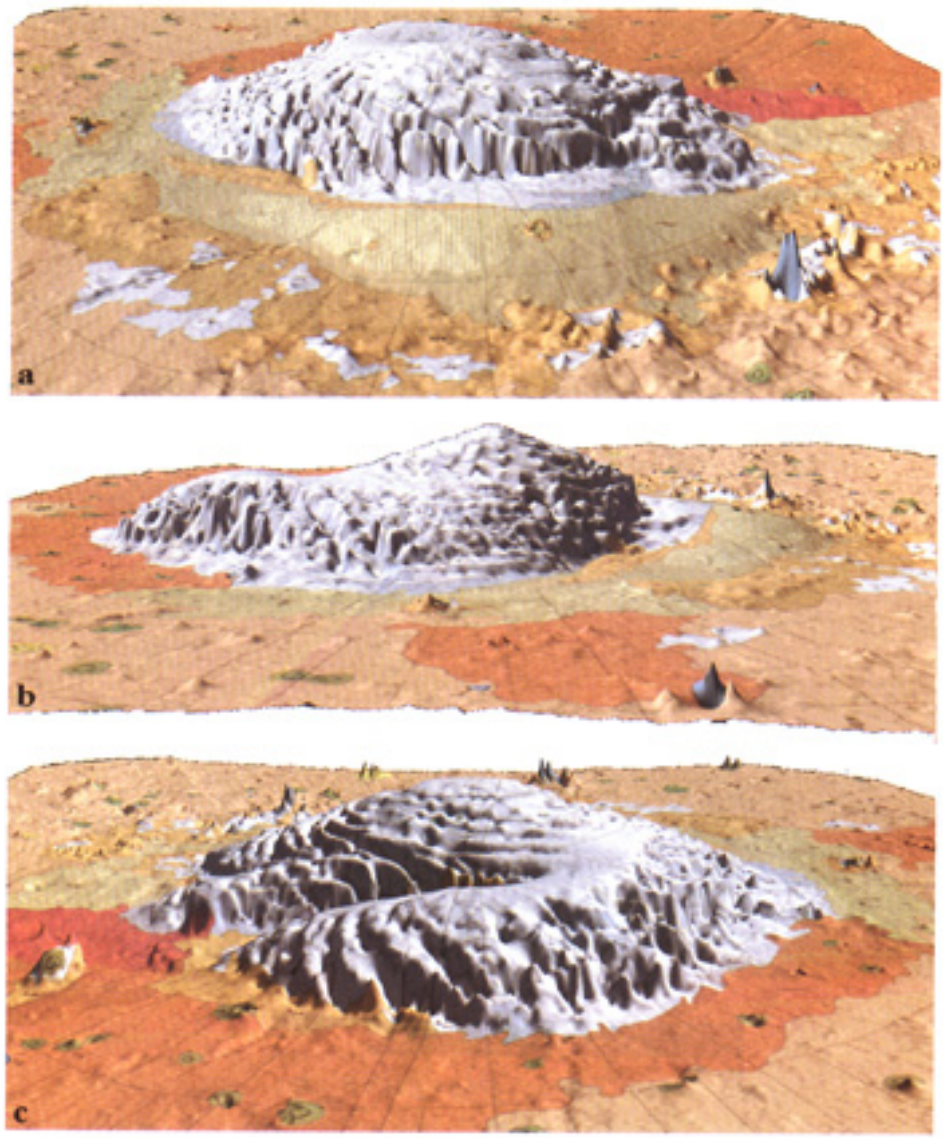

Plate 4. Perspective views of the geologic map of *Dial* [1994] created by superposing the map on MOLA topographic data. The irregularly shaped prominences and depressions associated with the low surrounding Olympia Planitia appear in Plate 4a, in which the view is from the 180° direction toward the pole. This low is occupied by mantled smooth plains. Some are mapped as outliers of polar material. The lobe of positive topography associated with Olympia Planitia and much of the north polar erg appears in Plates 4a and 4b viewed from the 270° direction toward the pole. The lowest parts of the North Polar Basin, occupied mainly by mottled cratered plains and mantled polygonal plains, are displayed in Plate 4c, which is viewed from the 360° direction toward the pole. Vertical exaggeration is 140x.

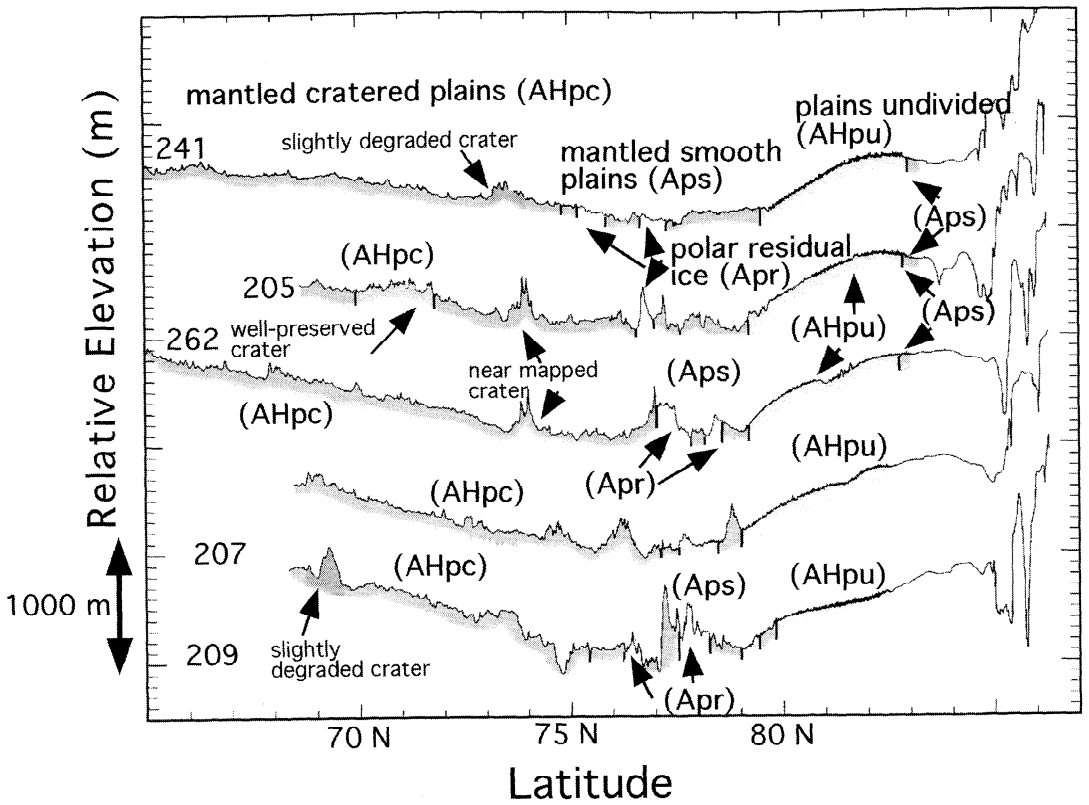

Figure 5. Annotated altimetric profiles (130° -180°; see plate 1): increasing negative slope of the mantled cratered plains (AHpc), the growing positive topography of the undivided plains (AHpu) (Olympia Planitia), and the presence of Aps and mapped polar material outliers within a slight depression between the dunes and the main cap. Smooth plains (Aps) also reside within a small low between Olympia Planitia and the cap. Olympia Planitia appears make the transition relatively smoothly into the topography of the main cap.

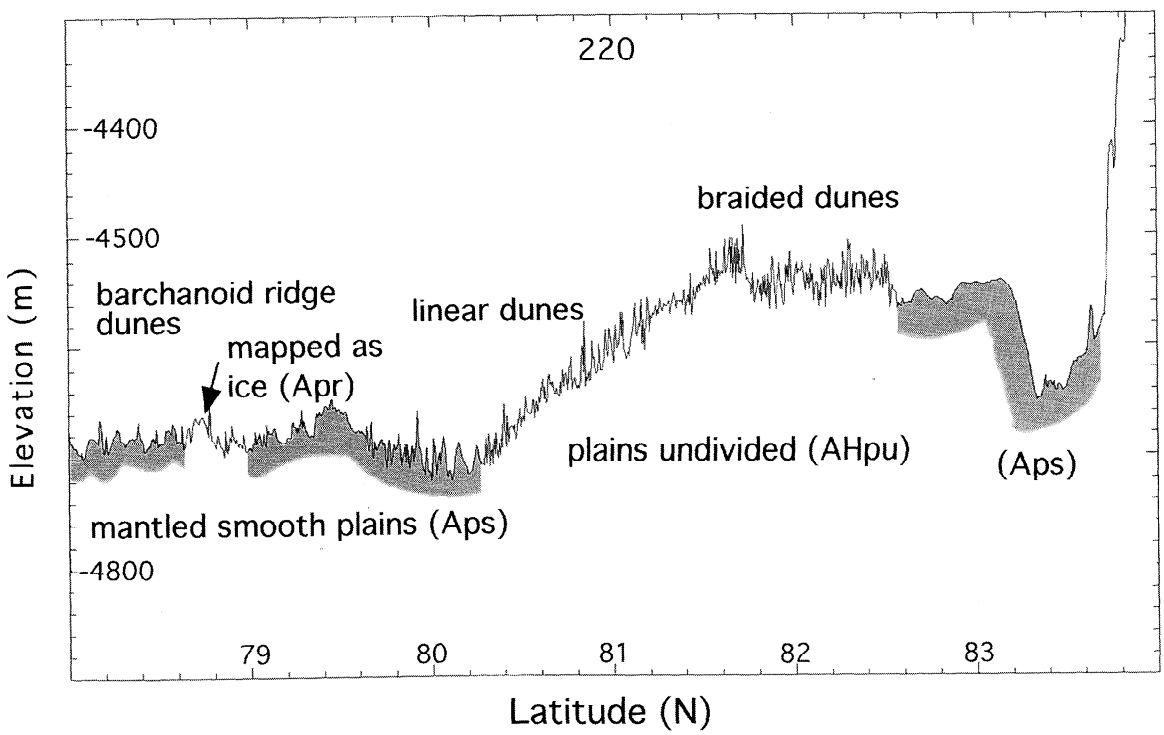

Figure 6. Annotated altimetric profile. High-resolution view (O220, Figure 4 of the transition from low-lying mantled smooth plains (Aps) to the increasingly positive topography of the undivided plains (AHpu) mantled by the high-frequency, short-wavelength topography of the dunes and then to the main cap. The smooth plains within a small topographic low show up here too. Vertical exaggeration is 300x.

ward of the undivided plains (AHpu) and is rougher than its counterpart at the base of the cap. The Aps, or Am, appear to be collecting, possibly by eolian redistribution, in flat, low-lying topography, overlying the mantled cratered plains (AHpc), or Hvk and Hvm.

At ~215°W (orbit 220), the undivided plains (AHpu) begin to slope systematically up toward the polar materials. This is well-demonstrated in orbit 220 (Figures 4 and 6) where AHpu, *Tanaka and Scott*'s [1987] lineated dunes in Olympia Planitia, begin to slope (~0.02°) upward toward the pole with a convex upward shape (slope ~0.12°). This is seen even more prominently in orbit 203, and as one moves toward the east, the convex-upward profile typical of this section of the circumpolar deposits is very striking (orbits 241, 205, 262, 207, and 209) (Figure 5). Instead of being a flat plain and basin that is collecting eolian sediment [e.g., *Breed et al.*, 1979], Olympia Planitia is a prominent positive feature sloping upward toward the pole.

As one proceeds to the east, the mantled cratered plains (AHpc) dip more steeply down toward the north pole and exhibit more prominent positive topography and depressions than in the previous profiles. The convex-upward shape of Olympia Planitia, with a slope of ~0.12°, is also becoming more and more prominent (orbits 203-241 and 205) at the base of the polar material, growing in its topographic expression and becoming indistinguishable from parts of the polar cap (Apr/Apl) (orbits 262 and 207-209) (Figures 4 and 5). In addition, the detailed altimetry profiles reveal the short wavelength topography that characterizes the dunes on the undivided plains (AHpu) and illustrates the dramatic change from AHpu to smoother polar materials, even though there is no major break in topography (e.g., orbit 220) (Figure 4).

The topography of Olympia Planitia [e.g., *Zuber et al.*, 1998a] suggests that the undivided plains (AHpu) are mantling an extension of the polar materials, with plains material on the relatively steep slopes being mobile and forming dunes. Some of this dune material may thus have been derived from sublimation of the polar deposits, a conclusion also reached by *Paige et al.* [1994] using thermal inertia data. Barchan dune areas have a higher thermal inertia [*Paige et al.*, 1994] than the transverse dunes of Olympia Planitia, which may be partially due to the fact that these dunes are not mantling portions of the polar materials and may have been partially derived from other sources. The ergs of the north polar regions have a lower thermal inertia as a whole than other Martian dunes [*Paige et al.*, 1994], which may due to the availability of other sources for dune material, such as oceanic and outflow sediment, pyroclastic ash from Alba Patera, and sublimation lag.

In this same region the mantled smooth plains (Aps) again tend to lie in topographic lows both at the base of the ~0.06° slope (orbits 241, 205, 262, 207, and 209, between 75° and 79°N) (Figure 5) and between the dune mantle and the exposed polar materials.

An additional characteristic of this region is the presence of outliers of Apr, or Api, the residual polar cap ice deposit.

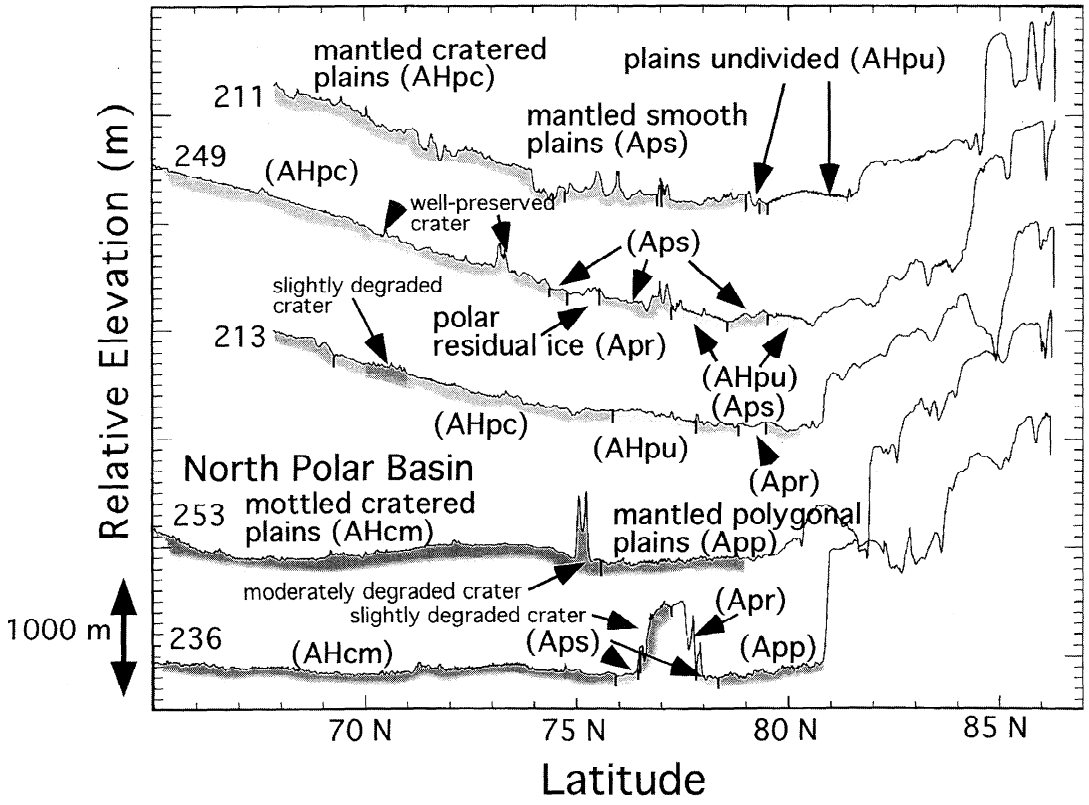

Figure 7. Annotated altimetric profiles (130° -180°; see Plate 1): transition of steeply sloping mantled cratered plains (AHpc) into the low-lying topography of the mottled cratered and mantled polygonal plains (App) on the lowest regions of the North Polar Basin floor. The flat to gently rolling topography of the AHcm contacts the relatively flatter topography of the App. App lies in juxtaposition with the steep scarp of the main cap in O236.

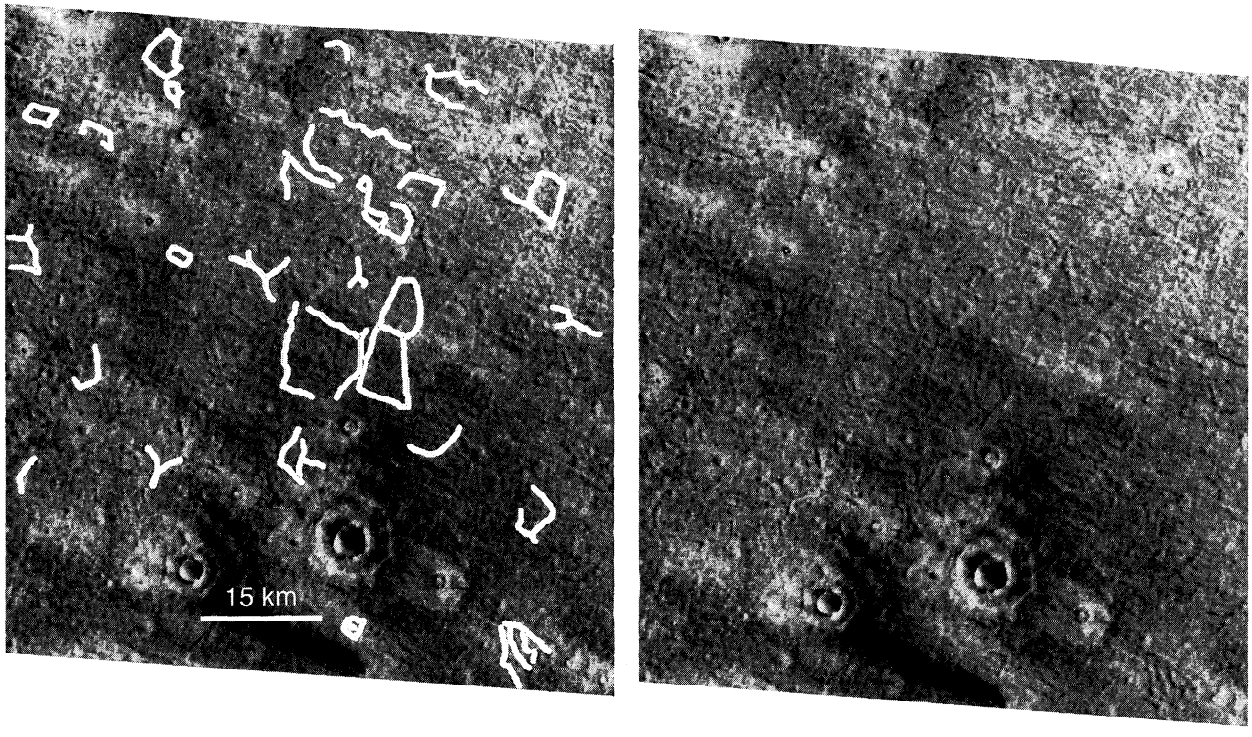

Figure 8. Viking image 701B20 (resolution ~194 m/pixel) showing subdued polygons within *Dial*'s [1984] mottled cratered plains (AHcm), south of the mantled polygonal plains (App) and within the North Polar Basin. The presence of these subdued polygons is consistent with App underlying part of AHcm. The ridged nature of these polygons may be due to infilling of polygonal troughs and later stripping. The polygons are outlined in the left-hand image.

Mapped in a band from ~220° to 105°W and 75° to 82°N, these deposits lie in the lowest parts of the circumpolar region in this area and are generally surrounded by mantled smooth plains (Aps or Am) (orbits 241, 205, 262, 207 and 209). These outliers exhibit a variety of topographic characteristics, which are discussed below.

Moving further eastward, the region from 105° to 90°W (orbits 211, 249, and 213) (Figure 7) shows a steeper slope (~0.10°) of the mantled cratered plains (AHpc) toward the north, with the number of possible craters decreasing, and a low area from about 75°-81°N dominated by undivided and mantled smooth plains (AHpu, Aps) and residual ice outcrops. In this region the prominent convex-upward area covered with longitudinal dunes decreases in lateral extent and topography, while the complementary sloping edge of the polar materials increases in lateral significance. Dunes are increasingly less evident, as the undivided plains (AHpu) are occupying flatter topographic regions. This is the transitional zone between the lowest parts of the North Polar Basin and the surrounding terrain, as shown in Plate 4c.

Beginning at ~80°-85°W, the lowest topography of the North Polar Basin is encountered (Plate 4c and Figure 7), and the geologic units change considerably. Mottled cratered plains (AHcm) replace the mantled cratered plains (AHpc). The topography of the region no longer slopes toward the north, but rather is relatively flat to broadly rolling (compare orbits 211, 249, and 213 to 253, 236, and 257) (Figures 7 and 9). Mantled polygonal plains (App) are exposed at one of the lowest points in the basin (orbit 253) (Figure 7), and exhibit a generally flat topography. In some places this polygonal terrain is juxtaposed with a relatively steep scarp forming the edge of the polar materials (Figure 7, orbit 236). *Tanaka and Scott*'s [1987] grooved member (Hvg) is exposed in a similar location to the patch of *Dial*'s [1984] mottled cratered plains (AHcm), centered at ~270°W, and near the mouth of Chasma Boreale within *Dial*'s [1984] mantled polygonal plains (App). The Hvg is the roughest of the Vastitas Borealis units, consistent with the presence of troughs and polygons on a scale of a few kilometers [*Kreslavsky and Head*, 1999]. The location of this grooved material is consistent with the mottled cratered plains (AHcm) centered at 270°W being of the same origin as those within the basin as discussed above.

In Viking images, subdued polygons are evident both within the mottled cratered plains (AHcm) in the basin and within the mantled smooth plains (Aps) at the mouth of Chasma Boreale [*Tanaka and Scott*, 1987; *Dial and Dohm*, 1994; *Fishbaugh and Head*, 1999, manuscript in preparation, 2000] (Figures 8 and 10). These observations suggest that the mottled cratered plains (AHcm), or Hvr, extend beneath some of the polygonal plains (App), or Hvg.

The mottled cratered plains (AHcm), or Hvr, and polygonal plains (App, Hvg), lying in some of the lowest topography of the Northern Hemisphere, may consist of fluvial sediment from Chryse outflow channels [*Baker et al.*, 1992] and possible standing bodies of water [*Parker et al.*, 1993] which have been deposited on top of the background sloping mantled cratered plains (AHpc), or Hvk and Hvm. *Hiesinger and Head* [2000], on the basis of MOLA data, favor a model of polygon formation which combines desiccation, shrinkage, unloading, and volume changes. The varying roughness values, with patches

of smooth and rough terrain at various wavelengths, within the North Polar Basin [*Kreslavsky and Head*, 1999] and the low-albedo and high-thermal inertia similar to intracrater dune deposits at lower latitudes [*Paige et al.*, 1994] imply a complex sedimentation and modification history. The stratigraphic relationship between the polygons and cap implies that the current polar cap was formed after the possible former ocean [*Parker et al.*, 1993] and outflow channel floods [*Baker et al.*, 1992] had disappeared. Roughness data composed of median slope values calculated on a baseline of 0.4-25 km is consistent with this observation. *Kreslavsky and Head* [1999] have shown that the cap is free of steep slopes except within Chasma Boreale, some troughs, and the cap edge. These observations imply, according to the authors, that the ice cannot withstand steep slopes and that existing steep slopes are young or still forming.

The flat mottled cratered plains (AHcm) are prominent until ~20°W (orbit 257) (Figure 9), where the contact turns north to ~73°-75°N. Mantled cratered plains (AHpc), or Hvk and Hvm , become prominent again, while mottled cratered plains (AHcm), or mantled plains (Am), are exposed in a narrow band between 75° and 78°N. In this region, there is almost no topographical distinction between the mottled cratered plains (AHcm), or Am, and the mantled cratered plains (AHpc), or Hvk. The sediment cover (AHcm) interpreted to lie on top of the mantled cratered plains (AHpc) thus appears to thin in this region.

In this same region, mantled smooth plains (Aps) are again found at the base of the cap (Figure 9) but are not as flat as those in previous profiles (see orbits 257 and 221 versus orbits 241, 205, and 262). In many profiles it is evident that where mantled smooth plains (Aps) or undivided plains (AHpu) do not lie at the base of the cap, the elevation difference between the cap and surrounding terrain is much more prominent than in the other case (i.e., compare orbits 246, 210, 229, 253, 236, 223, and 208 to 267, 233, 218, 213, 257, and 221), further suggesting that some of these plains units are mantling parts of the polar materials. The greatest lateral extent of polar layered terrain at the edge of the cap is also found in this region and has a high, steep topography, again indicating that the cap consists mainly of Apl.

In Figure 9, the profiles transect Chasma Boreale. *Dial* [1984] maps the Chasma as being occupied by mantled smooth plains (Aps), *Tanaka and Scott* [1987] map layered material and some crescentic dunes (Adc), and *Dial and Dohm* [1994] map mantle material and dunes. The material occupying the floor of the Chasma is seen to lie at a wide range of elevations but generally above those in the surrounding North Polar Basin. The Aps, which terminate in a lobe structure at the mouth of Chasma Boreale, have been observed to overlie the polygonal plains [*Fishbaugh and Head*, 1999, manuscript in preparation, 2000]. A Viking image (560B63) of part of the sediment lobe at the Chasma mouth is shown in Figure 10. The scarp visible on the right side of the image is part of the polar layered terrain that curves west from the Chasma wall (direction up the Chasma indicated by the arrow). A smaller scarp, on the western side of the sediment lobe, runs southwestward from the Chasma wall scarp, is interrupted by slump

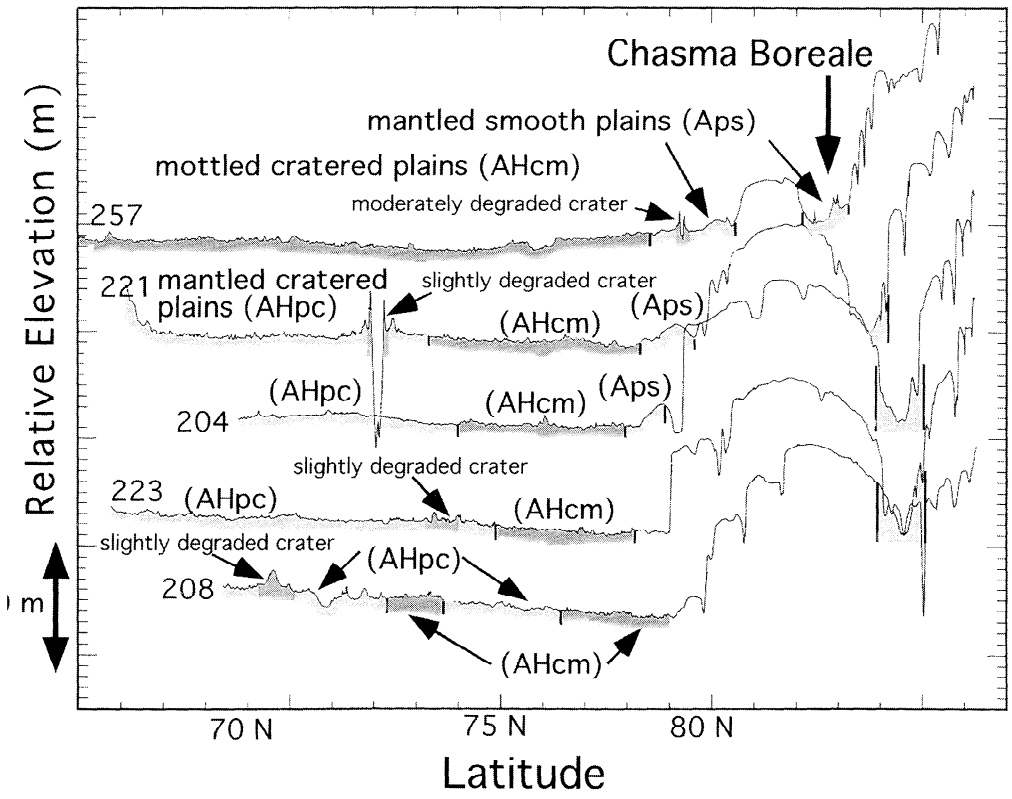

Figure 9. Annotated altimetric profiles (315° -25°; see Plate 1): gradual transition from the flat mottled cratered plains (AHcm) of the North Polar Basin floor to the gently rolling topography of the mantled cratered plains (AHpc), the appearance of mantled smooth plains (Aps) apparently draping the base of the cap, and Chasma Boreale whose floor is occupied by mantled smooth plains (Aps).

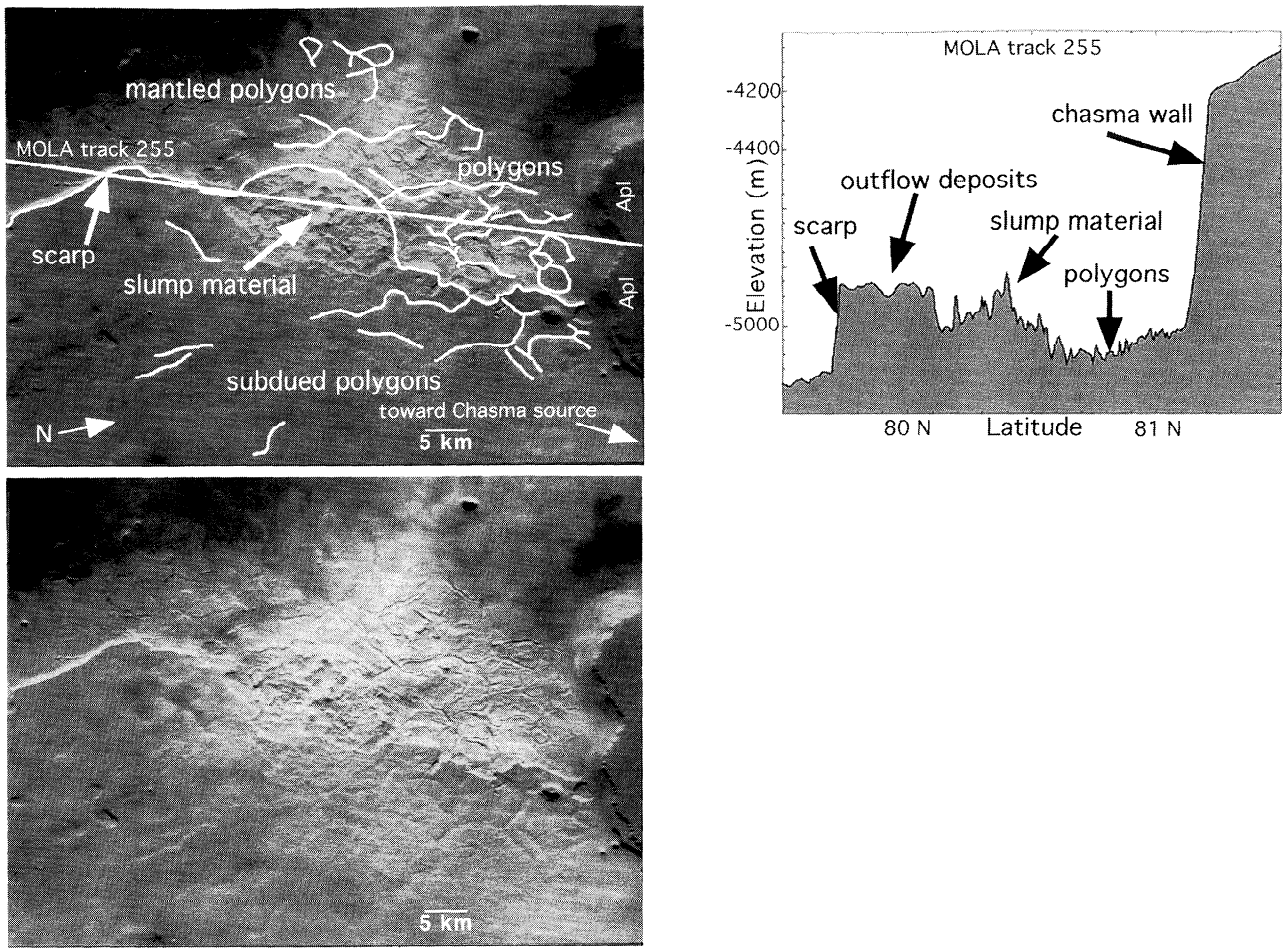

Figure 10. (a) Viking image 560B63 (resolution ~115m/pixel) showing possible jökulhlaup deposits at the mouth of Chasma Boreale [*Clifford,* 1987; *Benito et al.*, 1997; *Fishbaugh and Head,* 1999, manuscript in preparation, 2000] and underlying polygons of *Dial*'s [1984] mantled polygonal plains, App (*Tanaka and Scott*'s [1987] grooved member, Hvg). The annotated image outlines the Chasma wall, the scarp separating a region of subdued and better-defined polygons, and slump material from the scarp overlying the polygons. The material in which the scarp has formed is part of a lobate, possibly jökulhlaup-derived deposit extending from the mouth of the Chasma. The presence of subdued polygons beneath the flood deposits suggests that the deposits overlie the polygons. (b) Altimetric profile crossing (a) which shows the Chasma wall, with a slope of ~5°, the polygons, slump material, and scarp with a slope of about 9°. The height of the scarp at the point crossed by the profile is 150m and is higher than the scarp adjacent to the polygons, indicating that the polygons which have depths in Utopia Planitia ranging from 5 to 110 m [*Hiesinger and Head,* 2000] are able to appear in subdued form through the flood deposits.

material which overlies some of the polygonal plains (App), then becomes a scarp again, dividing a region of subdued and more defined polygons. A profile that crosses the image is also shown in Figure 10. The polygons, slump material, and scarps are evident in this profile. The height of the lobe scarp is small enough to allow polygons beneath the Chasma deposits to appear, in muted form, at the surface of the deposits.

These observations suggest that the deposits at the mouth of Chasma Boreale were deposited on top of the surrounding polygonal terrain, mantling and subduing the polygons and later slumping on top of them. These deposits may have resulted from the outflow of meltwater which may have carved Chasma Boreale [*Clifford*, 1987; *Benito et al.*, 1997; *Ross and Kargel*, 1998; *Fishbaugh and Head,* 1999, manuscript in preparation, 2000]. Near vertical scarps have been observed in glacial deposits and at the base of eroded avalanche fans associated with terrestrial jökulhlaup events [*Desloges and Church*, 1992].

These observations of the topography of the geologic units and unit contacts lead to formation of stratigraphic relationships between the units. Sketch cross sections of the stratigraphic relationships between the geologic units of both *Dial* [1984] and *Tanaka and Scott* [1987] based on this study are shown in Figures 14c and 14d. *Dial*'s [1984] cross section appears in Figure 14b. The main cap consists mostly of polar layered material (Apl) and is underlain by AHpu. Aps is within topographic lows. AHcm is gradational with AHpu, while AHpc is the same as AHcm, but mantled.

A new interpretation of the stratigraphy of *Dial*'s [1984] units, based on this study, is shown in Figure 14c. The cap consists mostly of Apl. Aps has collected into topographic lows and may be derived from various sources. This topographic low may have been created through lithospheric loading by the formerly larger polar cap (*Johnson et al.,* 2000). The ergs of AHpu drape part of the polar materials and may consist of material from various sources which resides on

slopes and is thus mobile. Residual polar material remnants, consisting mostly of polar layered material, and possible terrestrial kettles analogs are within a topographic low existing in an arc around the cap centered at 180°W. Parts of AHcm underlie App and lie along the slopes of AHpc. Other parts of AHcm lie on top of App and within flatter regions of the topography. Both AHcm and App underlie parts of or the entire cap and may have been derived from fluvial and/or oceanic sediments. AHpc underlies all other units and overlies the Noachian cratered surface.

Tanaka and Scott's [1987] stratigraphic column appears in Figure 2. Apl underlies Api, and dunes (Adc, Adl) and mantle material (Am) are formed at the same time as the polar materials (Api, Apl). The Vastitas Borealis Formation underlies the polar materials, dunes, and Am. Hvm is gradational with the other members. Hvr is gradational with Hvk and Hvm. Hvk began forming before the other members.

A sketch cross section of the stratigraphic relationships between *Tanaka and Scott*'s [1987] units based on the results from this study is shown in Figure 14d. The cap consists mostly of Apl. Adc and Adl lie along slopes (like AHpu), with Olympia Planitia (mostly Adc) draping parts of the cap (like AHpu). Am has collected in topographic lows (like Aps) and along Hvk and Hvm slopes (like parts of AHcm). Hvr and Hvg are gradational with each other and underlie the cap, forming analogous units to App and the parts of AHcm containing ridged polygons. Hvk and Hvm underlie the other units and overlie the ancient cratered surface (like AHpc).

3.3. Outliers of Polar Cap Material

We have used MOLA altimetric data to better constrain the nature and distribution of mapped polar material outliers. For the purposes of this study, we have located the mapped outliers [*Dial*, 1984] on the MOLA profiles described above. We first examined the outliers on the basis of comparison of topographic profiles. We then examined Viking images of the 14 mapped outliers appearing in the profiles in Figures 1-3, 5, 7 and 8 to further characterize these features and to identify those possibly associated with craters.

The mapped [*Dial*, 1984] polar material outliers and depressions lie within an arc from ~75° to ~80°N and ~95° to ~255°W. For the most part, mantled smooth plains (Aps), occupying a broad topographic low, surround the outliers. In the region subtended by the outlier arc, the terrain surrounding the cap slopes (~0.08°) toward the cap beginning at 65°N (the map limit) to ~75°N and flattens (although it is rough), then the Olympia Planitia region again slopes (~0.12°) upward toward the cap. It is in this flattened region that the mapped outliers lie (e.g., Plates 4a and 4b, and Figure 5).

3.3.1. Examples of outliers in profile. Examples of outliers in profile (Figure 11) show that some outliers have a prominent positive topography, some with positive topography are only partially mapped, some exhibit no positive topography, and some are depressions.

The mapped outliers with a positive topography (e.g., Figure 11) are distinguishable from the surrounding terrain by their height, width, and roughness. Some positive outliers have steeply sloping sides, while others exhibit more gradually sloped but rough sides. Features with a positive topography similar to those of the mapped outliers in the stacked profiles were identified in other profiles; these profiles were checked against the *Dial* [1984] map and against the 1.75 km resolution Viking mosaic to ensure that no mapped crater rims or craters visible on the scale of 1.75 km have been included. The following measurements are general estimates and are influenced partly by which part of the outlier the profile crosses. The heights of the positive outliers range from ~75 to ~775 m and average ~295 m with a standard deviation of ~155 m using a sample size of 24. The widths of the outliers range from ~15 to ~90 km, averaging ~50 km with a standard deviation of ~20 km.

Their size, which distinguishes them from seasonal frost patches, and their topographic distinctiveness from the surrounding plains imply that these prominences are indeed polar material outliers. The rougher surface of the outliers on a smaller scale as compared to the main cap and the surrounding terrain [*Kreslavsky and Head*, 1999] could be due to continual deposition of ice and frost on the surface of the main cap and to differing effects of erosion on the ice of the outliers versus the deposits of the surrounding terrain.

An example of a prominence partly mapped as a polar material outlier [*Dial*, 1984] is shown in Figure 11b. If a positive outlier has been identified in profile but has not been mapped or has only been partially mapped, it may be that the feature is an outlier of polar layered terrain with a moderate albedo due to a higher concentration of dust. *Tanaka and Scott* [1987] have mapped outliers of polar layered materials within the North Polar Basin and in the outlier arc region. As described below, some mapped positive outliers do have a moderate albedo, which may indicate that they consist of polar layered material with a higher dust concentration. The fact that layered terrain may constitute most of the cap, as discussed above, further substantiates the possibility that unmapped or partially mapped outliers consist of layered terrain with a higher dust concentration. The outliers in the circumpolar outlier arc region have very high thermal inertia, as does the main cap, suggesting that they are composed of water ice or snow at least from a few millimeters below the surface to 20 cm below the surface [*Paige et al.*, 1994]. Additional possibilities are that part (or all) of the outlier is mantled by dust or sand, which would mask the existence of the ice in albedo images or that material has been deposited against the prominent outlier. The fact that some outliers of prominent positive topography are not mapped or only partially mapped suggests that the number of polar material outliers is more extensive than has been previously mapped.

Flat regions that have been mapped as polar material outliers (Figure 11c) may represent regions of seasonal frost. Of the 14 mapped outliers shown in the profiles in Figures 3-5, 7, and 9, three have a generally flat topography (orbits 214, 220, and 241). Thermal inertia data suggest that thin layers of frost are deposited seasonally, changing shape and extent from season to season [*Paige et al.*, 1994].

The depressions (Figure 11c) occur in similar locations to the outliers with positive topography but are greater in number. The depressions, in general, have rough floors. Some depressions exhibit rougher sides. The slope of the sides averages ~0.3°. The average depth/diameter ratio is ~0.005. These depressions can be distinguished from typical, fresh craters in that they exhibit little or no rim topography, are generally shallower relative to their diameter than observed Martian north polar craters [*Garvin and Frawley*, 1998; *Garvin et al.*, 1998, 2000], and are not circular in shape (see below). The depth of the depressions ranges from ~50 to ~650 m and averages ~200 m with a standard deviation of ~125 m using a sam-

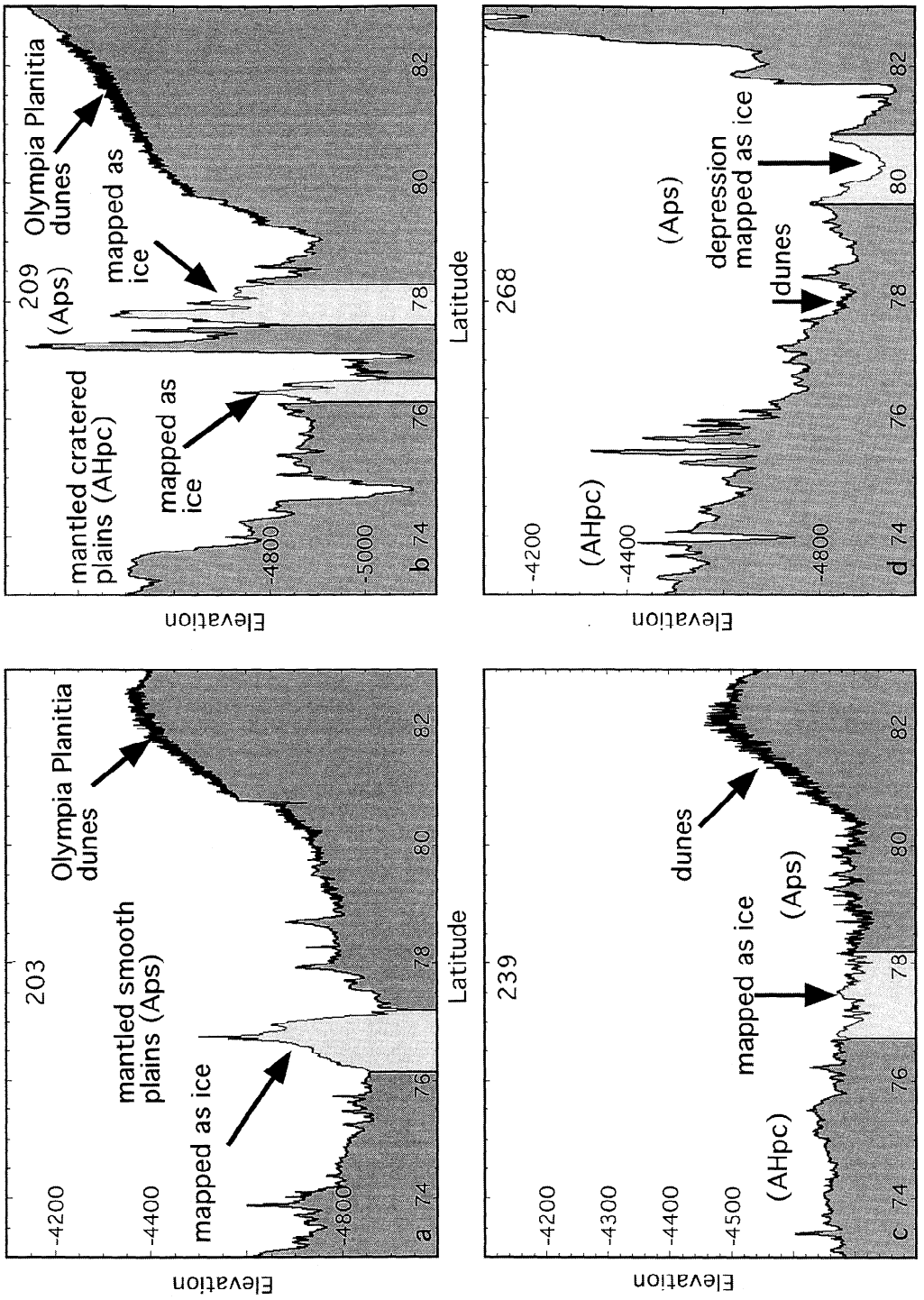

Figure 11. Polar cap material outliers in profile. The mapped outliers are in light gray. These outliers exhibit a variety of topographic characteristics. (a) Some have a prominent positive topography and thus may be patches of remnant polar material. (b) Some positive topographic features are only partially mapped as outliers; these may have material piled at the base, may be partially mantled by dust, or may consist partly of polar layered material. (c) Some are flat, which may be seasonal frost patches. (d) Some appear as depressions and thus may be analogous to terrestrial kettles. Vertical exaggeration is 494x.

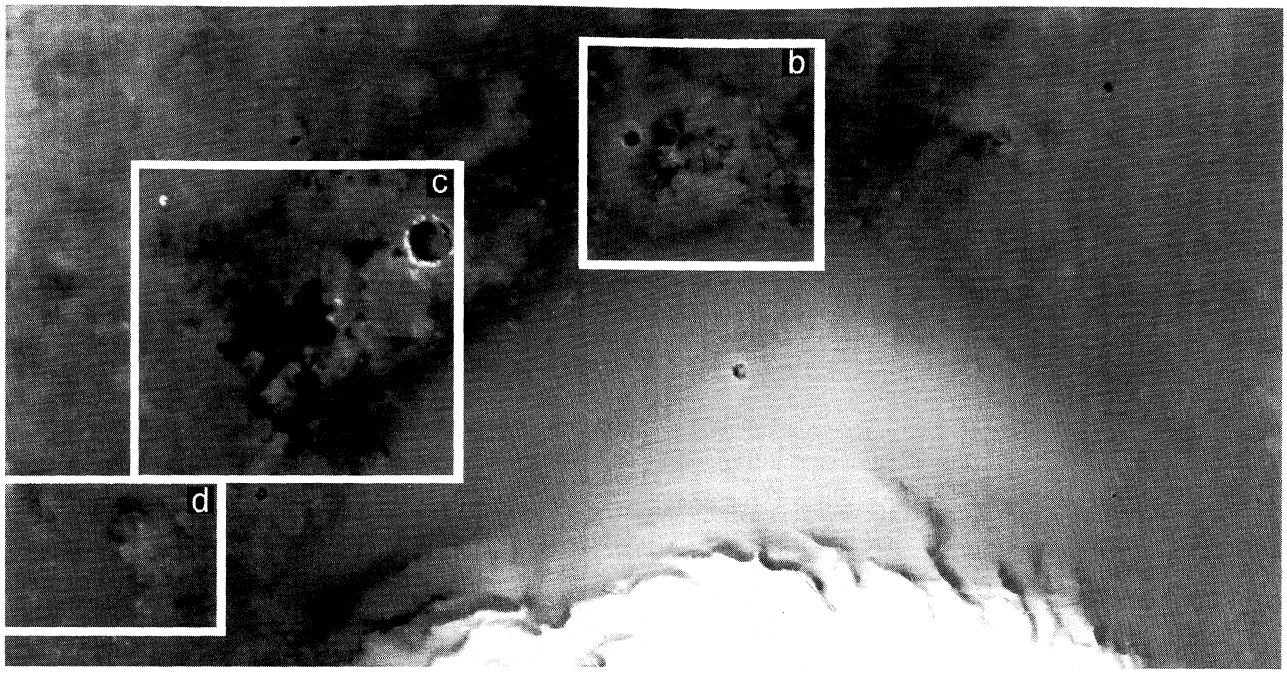

Figure 12. (a) Topographic map enhanced to show details of the outlier arc region. This region exhibits a marked topographic distinction from the surrounding mantled cratered (AHpc) and mantled smooth (Aps) plains. The close-ups in Figures 12b – 12d are outlined as boxes. (b) Close-up of topography and associated profiles. There is a large, irregularly shaped depression in the center and mesas which can be contrasted to the ~18 km diameter crater which was mapped by *Dial* [1984] as ice. Profile 262 (vertical exaggeration 230x) crosses some of the ejecta of the crater and can be contrasted to profile 372 (vertical exaggeration 180x) which crosses the depression and mesas and exhibits a hummocky and knobby topography. (c) Large depressions and mesas near a ~47 km diameter crater. MOLA profile 393 (vertical exaggeration 81x) crosses the crater, and profile 209 (vertical exaggeration 277x) crosses the depressions and mesas. The profiles of the depressions and mesas can be contrasted to the distinct crater profile. (d) Close-up of a mesa in the outlier arc region. Note that the mesa, near mapped ice [*Dial*, 1984] does not appear to be associated with a crater, does not have a regular shape, and has a prominent topography compared to the surrounding plains. Profile 433 has vertical exaggeration of 277x.

ple size of 28. The width of the depressions ranges from ~15 to ~75 km, averaging ~45 km with a standard deviation of ~15 km. An example of a depression appears in Figure 9d. The depressions may represent residual ice or frost-filled craters and analogs to terrestrial kettles. On the basis of their larger size and proximity to the polar cap, we interpret these features to be different than the smaller, irregular depressions in Acidalia and Utopia Planitia interpreted by *Costard and Kargel* [1995] to be thermokarstic features formed in ice-rich outflow channel sediment.

3.3.2. Topographic map of outlier region. A detailed topographic map within the outlier arc region (Figure 12a) shows that the eastern half of the outlier arc region appears to be quite rough, as also observed by *Kreslavsky and Head* [1999], while the western half of the arc has very little topographic signature and probably represents mostly seasonal frost outliers. The western half also has a higher thermal inertia and albedo [*Paige et al.*, 1994], which may be due either to the presence of seasonal frost in this region or to the mantling on the eastern outliers of pyroclastic ash from Alba Patera. The rougher region has irregularly shaped depressions, mesas, and knobs, appearing morphologically distinct from typical background cratered plains and being too numerous to represent craters. Knobs are visible within depressions. One crater, centered at (77°N, 165°W), has been mapped as a polar material outlier [*Dial*, 1984]. The depressions and positive topography can be contrasted with the few craters visible in the map in this region. Close-ups of the topography and associated representative topographic profiles appear in Figures 12b-12d.

Depressions and mesas contrasted with a small crater are shown in Figure 12b. This crater has been mapped by *Dial* [1984] as ice and may therefore have been covered by frost in images used for mapping. The large depression to the south of the crater exhibits a noncircular shape, has small knobs and mesas within it, and is surrounded by higher topography. Orbit 262 crosses the ejecta of the crater. Orbit 372 crosses the depression and knobs and mesas. The topography is rougher than the crater ejecta on a vertical scale of hundreds of meters and looks much like the high topography of orbit 209 in Figure 12c. This rough topography is not associated with any circular features and is quite distinguishable from the surrounding plains.

The irregular nature of the depressions and mesas in the outlier arc region is also illustrated in Figure 12c. A large depression lies in the middle of the figure with many smaller depressions and higher topography surrounding it. These can be contrasted with the ~60 km diameter crater and the smaller crater adjacent to it in the upper right-hand corner of the figure which show well-developed rims and circular shapes. Orbit 209 shows a profile that crosses cratered plains, the large depression, mesas, and one smaller depression. Some of the terrain crossed by this profile has been mapped by *Dial* [1984] as outlying ice. The rough outlier region can be contrasted with the cratered plains that show much less topographic variation.

Orbit 393 crosses a knob, small irregular depressions, and the larger crater. The crater exhibits obvious rim structure which depressions in Orbit 338 do not show.

A close-up of a mesa in the outlier arc region is shown in Figure 12d. The mesa does not appear to be part of a crater rim and does not exhibit a regular shape. The mesa is obvious in the profile, rising steeply above the surrounding plains. A small crater with a well-developed rim may exist on the northern side of the mesa. This mesa lies near mapped ice. The size of this mesa, its distinction from the plains, and its location near mapped ice suggest that this is indeed an outlier of polar material.

These observations show that the outlier arc region is characterized by rough topography distinguishable from the cratered plains and not completely defined by craters, leading to the possibility that the topography in the outlier arc region may consist in part of remnants of polar material and that terrestrial kettles may represent an analog to some of the depressions. Ablation of glaciers can leave behind buried blocks of ice which later melt, leaving kettle holes [*Flint*, 1963; *Clark*, 1969; *Benn and Evans*, 1998]. On Mars, sublimation rather than (or in addition to) melting may be the dominant ablational process.

3.3.3. Examples of outliers in Viking images. Examples of images of outliers displayed in the stacked profiles in Figures 3-5, 7, and 9 taken from the 1.75 km resolution Viking mosaic are displayed in Figure 13. This mosaic was created by using images taken at different times of the Martian year. Each image is labeled by orbit number. The mapped outlier lies between

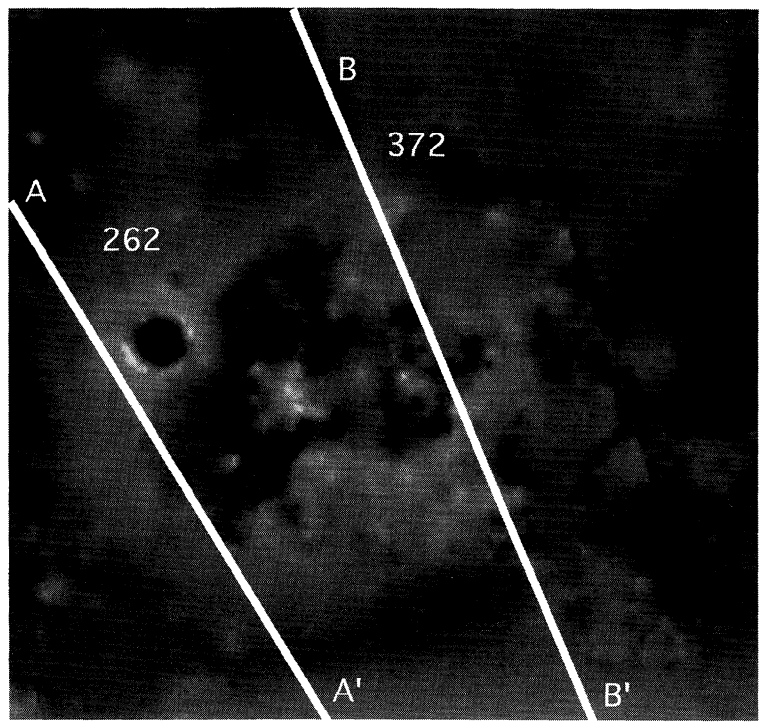

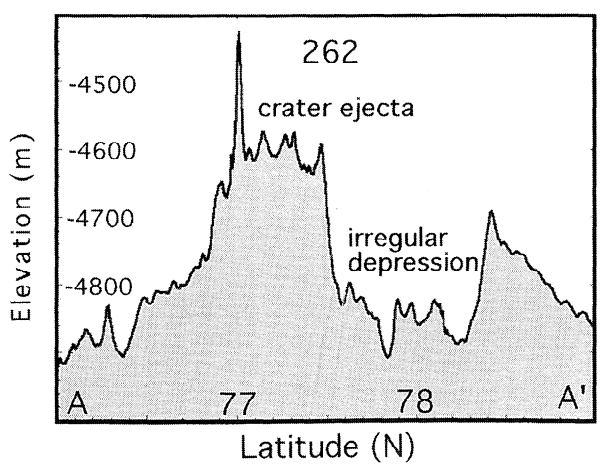

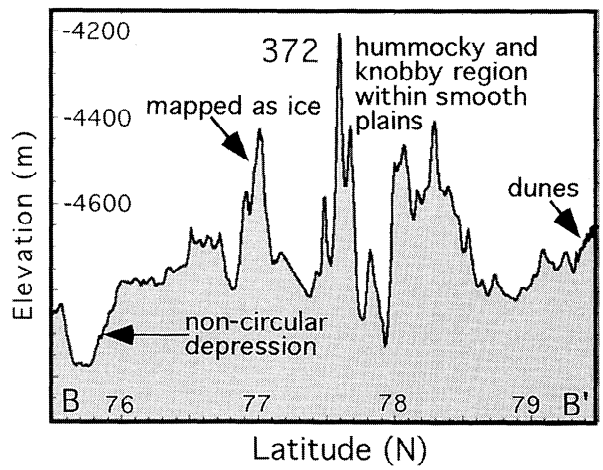

Figure 12. (continued)

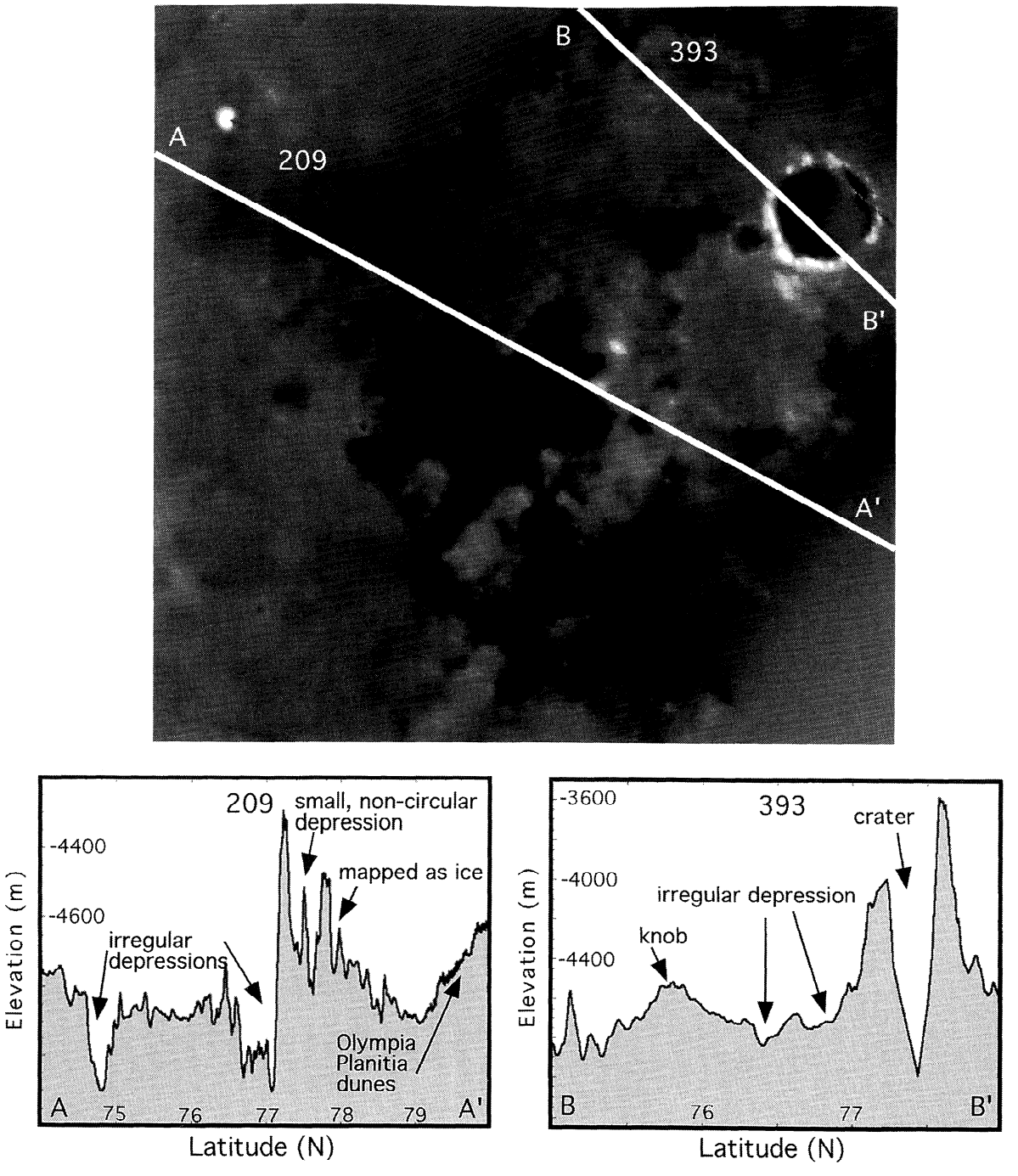

Figure 12. (continued)

the white arrowheads. In the following discussion we refer to outliers by orbit number.

Outlier 214, which has a diameter of ~30 km, lies near a ~30 km diameter crater. One of the outliers in orbit 220 is associated with a bright patch, and one lies within mottled light and dark terrain; no craters are visible. Outliers 203 and 241 lie within a bright patch, and no craters are visible. Outlier 205 lies within a bright patch. A small darker feature, which may be a degraded crater, can be found just above the bottom arrowhead, but the outlier is almost three times the size of this feature (~8.75 versus ~24.5 km). Outlier 262, which is ~30 km in diameter, lies near a ~20 km diameter crater. Outlier 209 is part of a bright patch surrounded by low-albedo terrain. Outlier 249 is also part of a bright patch with no visible craters. The outlier in orbit 213 is not associated with any bright patches (the nearest are ~90 km away), and no crater is visible.

These images suggest that while some mapped outliers and those prominences and depressions identified in profiles may actually be polar material outliers and kettles, others may actually be craters covered or filled with ice and/or frost. There are several possible reasons for this coating or filling, which could exist in combination: (1) the craters and/or the surrounding terrain act as a cold trap, allowing seasonal frost to remain throughout the year; (2) the higher elevations of the

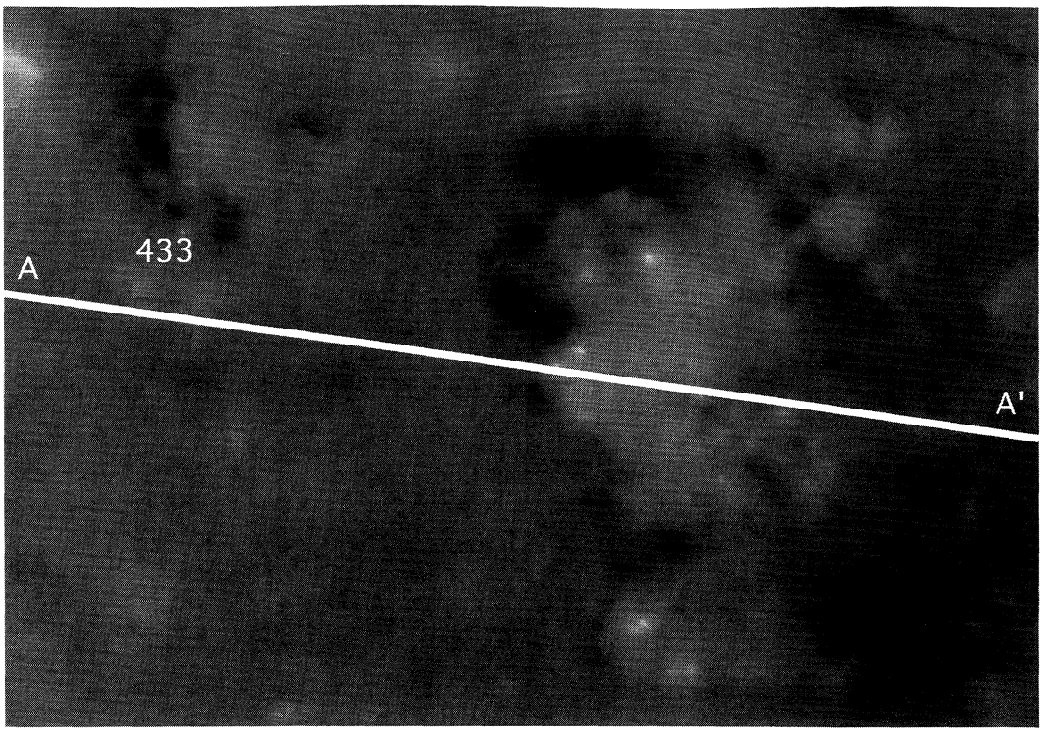

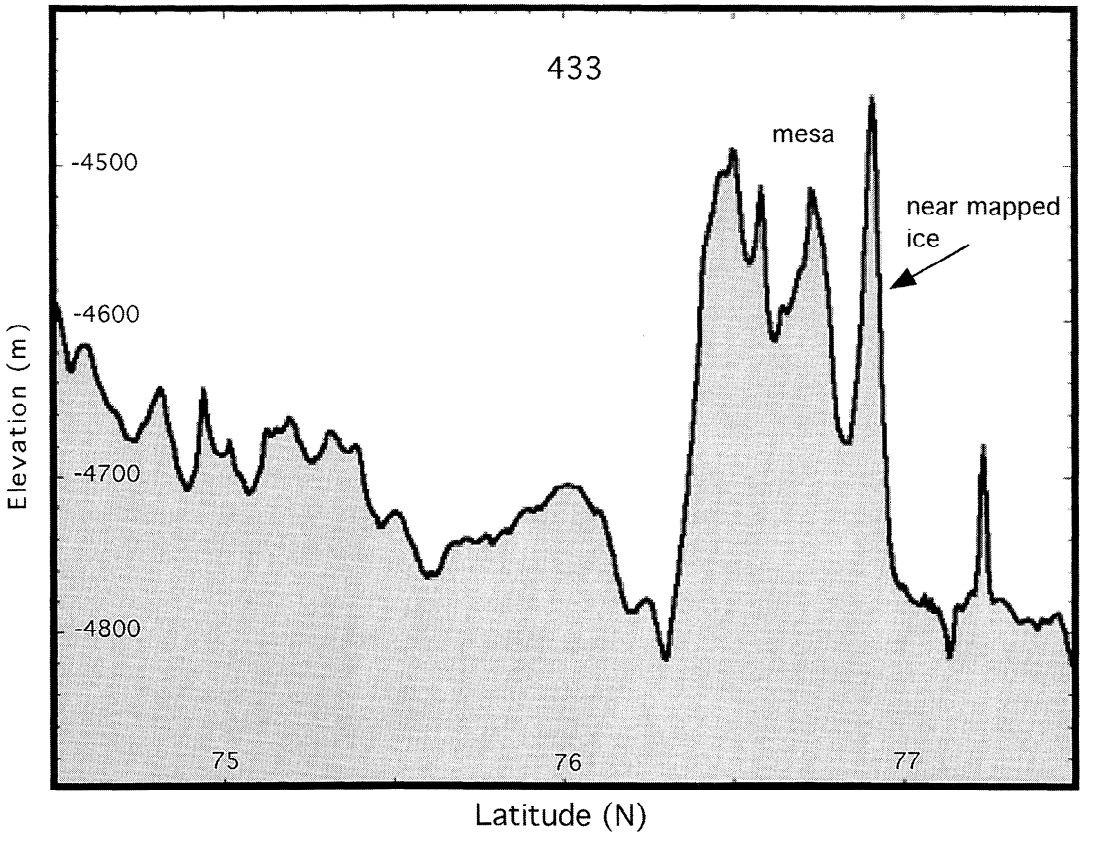

Figure 12. (continued)

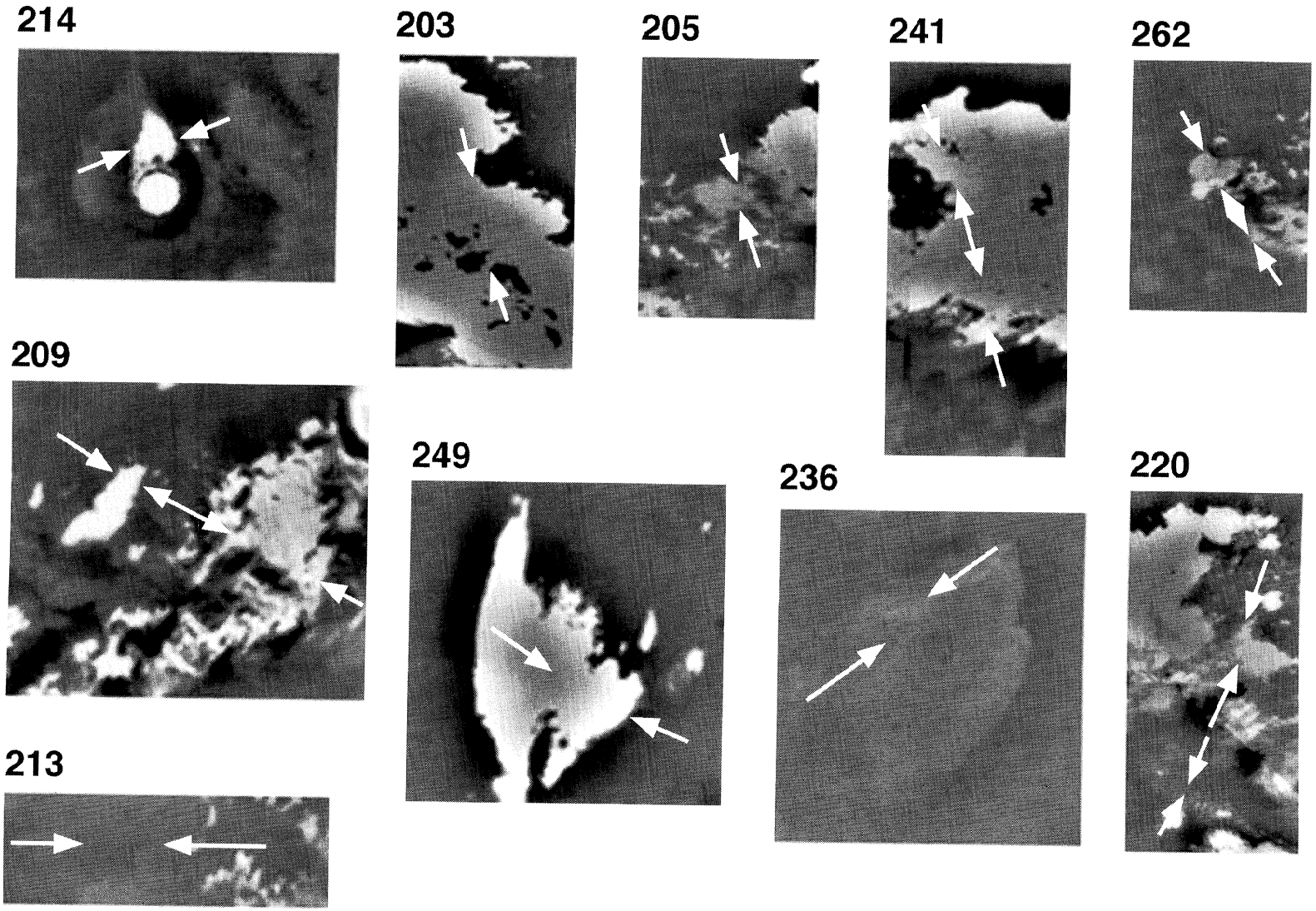

Figure 13. Examples of mapped polar material outliers in Viking images from a 1.75 km resolution Viking mosaic made up of images taken at different times of the Martian year. This plot shows both geological features mapped as residual ice deposits and seasonal volatile deposits. The mapped outliers lie between the arrowheads. Each image is labeled by MOLA profile number. Outliers 214 and 262 are associated with craters that also have seasonal frost. Outliers 249, 203, and 241 are associated with large patches of ice and frost. Outliers 236 and 213 have a moderate albedo possibly associated with layered terrain of ice and dust.

crater rims allow frost to remain frozen throughout the year; and (3) and the cap was once larger, including the mapped polar material outlier arc, and as the cap receded, craters acted as cold traps, allowing ice to remain. *Garvin et al.* [2000] have observed that craters associated with ice and frost deposits show topographic evidence of infill. The authors propose that these craters could have been filled by ice and dust sedimentation during times of polar cap advance or that the craters were buried by ice and sediment and later exhumed.

D. Bass et al. [2000] have examined Mariner 9 and Viking images and found that the shape of the outliers in late summer does not change significantly from year to year, which was interpreted to mean that the outliers lie within cold traps created by the topography. However, MOLA topographic data indicate unique topography not always associated with craters; thus the fact the outliers do not change shape further substantiates the conclusion that the outliers are composed of both frost or ice-filled craters and kettles and outliers of polar cap material. Of the 10 mapped [*Dial*, 1984] outliers examined in the 1.75 km resolution Viking mosaic, two are likely to be associated with craters (outliers 214 and 262), two are proposed to be associated with moderate-albedo layered terrain with a higher concentration of dust (outliers 213 and 236), and the remaining six are associated with bright patches of polar material and frost.

Tanaka and Scott [1987] have mapped outliers in similar locations to those mapped by *Dial* [1984] and have mapped additional outliers between 10°-70°W and 70°-80°N. *Tanaka and Scott*'s [1987] outliers are of a different shape than Dial's outliers, probably owing to varying amounts of mapping of seasonal frost. In general, most of *Tanaka and Scott*'s [1987] outliers are smaller than *Dial*'s [1984]. *Dial* [1984] has mapped the outliers as residual ice, while *Tanaka and Scott* [1987] have mapped residual ice and polar layered terrain outliers (e.g. the orbit 236 outlier, Figure 7). These differences in mapping further suggest that the mapped polar material outliers are indeed of mixed origin and that some of the mapped outliers having a moderate albedo may consist of layered terrain with a higher concentration of dust.

4. Conclusions

4.1. Topography: Implications for Stratigraphic Relationships and Geologic History

We describe below a preliminary model of the geologic history of the region from oldest to youngest, including both *Dial's* [1984] and *Tanaka and Scott's* [1987] units. Figure 14a shows *Squyres's* [1979] cross section of the polar deposits, Figure 14b shows *Dial's* [1984] generalized cross section, Figure 14c shows a revised generalized cross section of *Dial's* [1984] units based on this study, and Figure 14d shows a revised generalized cross section of *Tanaka and Scott's* [1987] units based on this study. *Tanaka and Scott's* [1987] stratigraphic column is shown in Figure 2. *Squyres et al.* [1979] have proposed that the layered deposits and debris mantle are formed by the same mechanism. Layered deposits consist of dust deposited onto perennial ice, and the debris-mantle sedi-

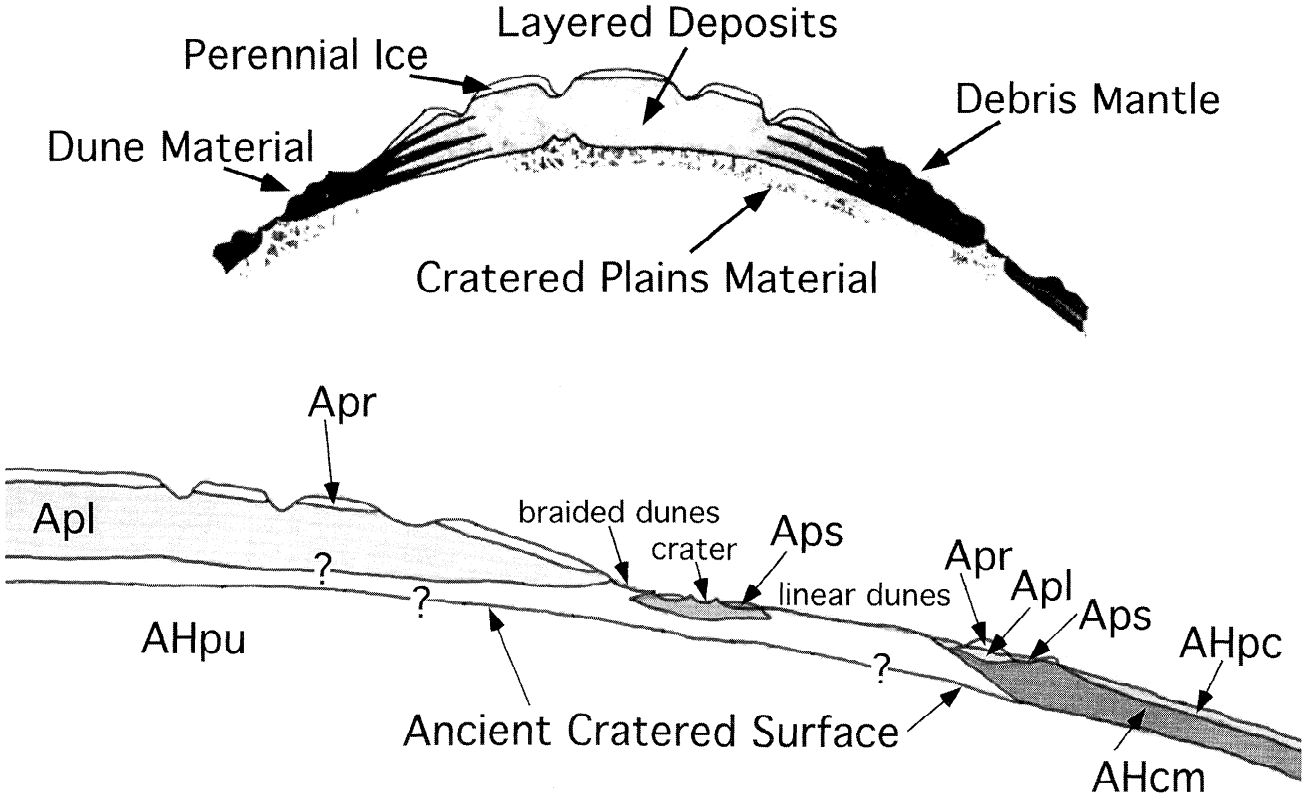

Figure 14. (a) Cross section of the north polar region as interpreted by *Squyres* [1979]. (b) Generalized cross section of the North polar region according to *Dial* [1984]. (c) A new generalized cross section, according to this study, of the stratigraphic relationships between *Dial*'s [1984] units. (d) A new generalized cross section of *Scott and Tanaka*'s [1987] geologic units using the results of this study. For *Scott and Tanaka*'s [1987] original stratigraphy, see the stratigraphic column in Figure 2.

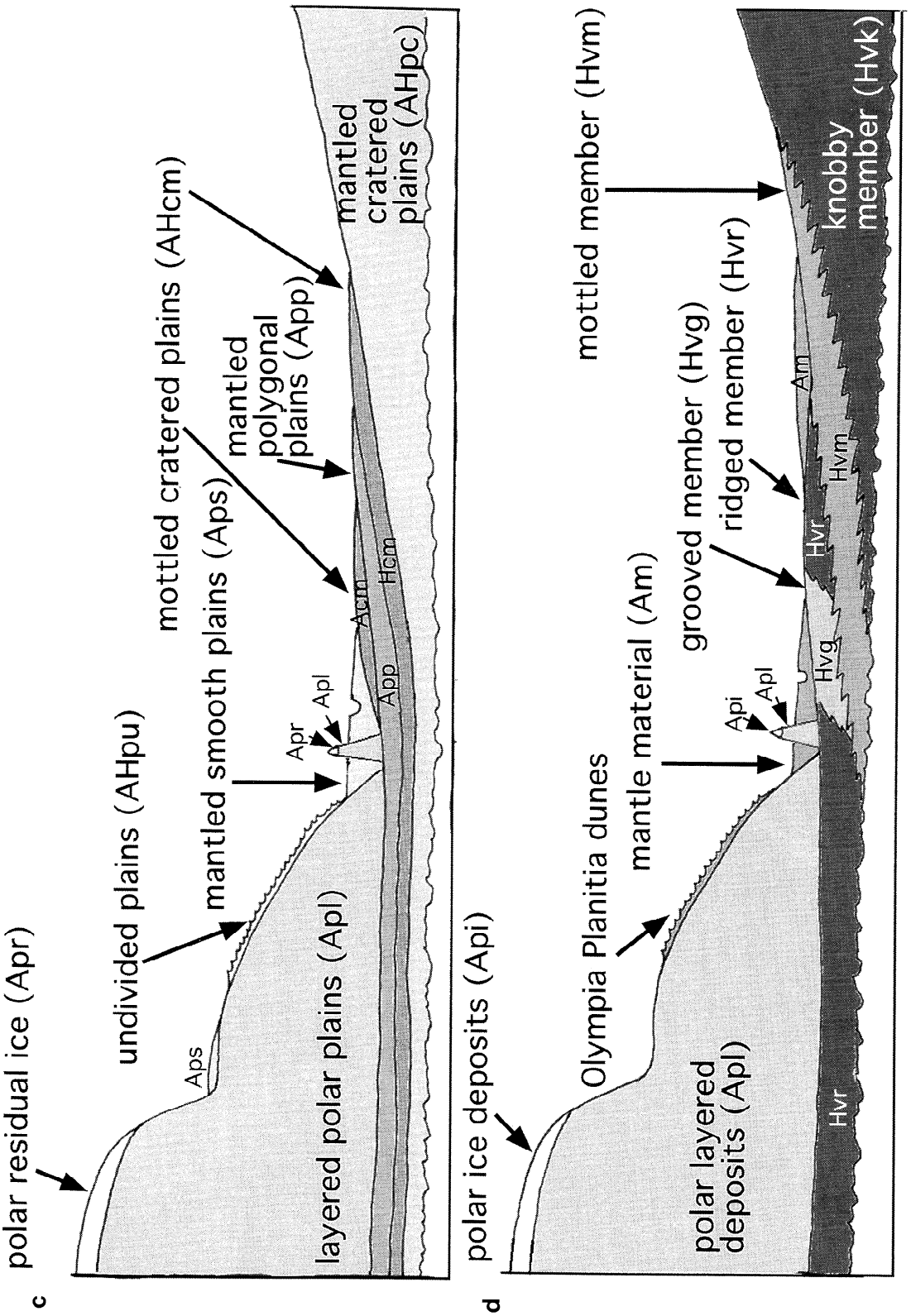

Figure 14. (continued)

ments have been deposited onto the surface of units surrounding the poles; they can be considered facies of the same unit. In this scenario, fluctuations in the lateral extent of the perennial ice margin caused by climate changes result in alternating periods of formation and erosion of the layered terrain and in the interfingering of the layered deposits with the debris mantle. This cross section is shown in Figure 14a.

Dial [1984] interpreted the mantled cratered plains (AHpc) to be of the same origin as mottled cratered plains (AHcm) (a permafrost crust consisting of water ice and volcanics) but with a mantle. *Tanaka and Scott* [1987] proposed that the knobby member (Hvk) of the Vastitas Borealis Formation is characterized by small volcanoes and degraded highland remnants and that the mottled member (Hvm) has domes that are either viscous lava flows or volcanoes that were also a source for some of the plains near Hvm. The topography is consistent with this latter interpretation. The knobby (Hvk) and mottled (Hvm) members of the Vastitas Borealis Formation mainly slope toward the pole, as do *Dial*'s [1984] mantled cratered plains (AHpc), suggesting that these plains provided a background for later sedimentation, underlying all other units in this map area and overlying the Noachian cratered surface.

Many authors have interpreted the mantled polygonal plains (App) to have resulted from a variety of mechanisms. *Dial* [1984] interpreted the App to lie stratigraphically between the mantled smooth plains (Aps) and the AHpc. The gently rolling and then flattening topography of the AHcm-App contact and the evidence of subdued polygons within both the Aps at the mouth of Chasma Boreale and within the AHcm in the North Polar Basin, analogous to *Tanaka and Scott*'s [1987] ridged member (Hvr), provide evidence that the App underlies the Aps and some of the AHcm. This observation is consistent with the interpretation by *Tanaka and Scott* [1987] that the grooved member (Hvg) exposed at the mouth of Chasma Boreale may be buried elsewhere. We suggest that the polygonal plains, occupying a flat, low-lying portion of the basin, may have been originally emplaced as wet outflow channel [*Baker et al.*, 1992; *Lucchitta et al.*, 1986] and oceanic sediments [*Parker et al.*, 1993]. Polygons formed in these deposits during subsequent desiccation. Some of this polygonal terrain has been exposed near the mouth of Chasma Boreale, possibly by the maximum stages of the flood that may have carved the Chasma [*Clifford*, 1987; *Benito et al.*, 1997; *Fishbaugh and Head*, 1999, manuscript in preparation, 2000]. The flat, low-lying topography of the App and Hvg at contacts with relatively steep edges of the polar deposits in some places suggest that they may underlie some of or the entire main cap.

The topography of the contact between the mottled cratered plains (AHcm) and the App, the crater age of the AHcm [*Dial*, 1984], and the presence of subdued polygons within the AHcm, are consistent with formation before, during, and after the polygonal terrain (App). Thus the AHcm, like the ridged member (Hvr), may extend beneath the cap, and the AHcm/Hvg region centered near 270°W may be an extension of those mottled plains within the basin. The similarity in roughness between these two regions [*Kreslavsky and Head*, 1999] supports a similar origin. The mantled plains (Am) of *Tanaka and Scott* [1987], or AHcm of *Dial* [1984], between 300° and 30°W form a thin fluvial sediment layer which lies along the slopes of AHpc. The AHcm may consist of a mix of volcanics [*Dial*, 1984], both local and from Alba Patera, and sediments deposited by a paleo-ocean and/or by outflow channels.

The high topography of the layered polar plains (Apl), their similar composition to that of the polar residual ice cap (Apr) as implied by thermal inertia data [*Paige et al.*, 1994], the moderate albedo of some polar material outliers, and the fact that *Tanaka and Scott* [1987] map some of the outliers as polar layered material suggest that the Apl constitutes most of the main cap and the residual polar material remnants. If the polar materials were formed on top of the polygonal plains, as suggested by the topography of the contact between these units, then the polar materials formed after the possible ocean had disappeared, indicating that the cap is relatively young. The similarity with the south polar deposits, in the presence of spiraling troughs and layered material [*Tanaka and Scott*, 1987] and in size [*Smith et al.*, 1999], also suggests that the north polar cap has not interacted with or been formed predominantly by a standing body of water or by outflow channels.

According to *Dial* [1984], the mantled smooth plains (Aps) originated from small volcanoes or other now buried sources. *Tanaka and Scott* [1987] propose that the mantled plains (Am) consists of seasonal eolian deposits and by - products of erosion of the polar layered material (Apl), of the ergs, and of the subpolar plains. The fact that the Aps, analogous to Am and linear dunes (Adl), lie within topographic lows implies that this sediment may have come from sources suggested by both mappers and has been transported by some process, probably mostly eolian, to fill these lows. The Aps may consist of a mix of volcanics, both local and from Alba Patera, reworked sediment from other plains units, and lag from sublimation of the layered deposits. Those smooth plains and crescentic dunes (Adc) within Chasma Boreale may have been derived both from sedimentation due to the catastrophic outflow that may have carved the Chasma and from sublimation of polar layered deposits.

Previous topographic maps [*USGS*, 1991] showed Olympia Planitia, the undivided plains (AHpu), to be a relatively flat plain, and the longitudinal dune deposits were interpreted to represent a large sand supply and to fill the lowland plain [*Breed et al.*, 1979; *Tanaka and Scott*, 1987; *Dial*, 1984]. MOLA data reveal, however, that most of this region is composed of positive topography that is convex upward and contiguous with the topography of the polar residual cap (Plates 3, 4a, and 4b and Figures 5 and 6). Thus we interpret this region to represent an extension of the polar cap materials now mantled by dunes. These dunes may consist of material derived from various sources, including sublimation lag from the layered deposits.

4.2. Polar Material Outliers

Polar material outliers mapped by *Dial* [1984] and *Tanaka and Scott* [1987] were identified using Viking Orbiter and Mariner 9 images. These outliers have been postulated to be remnants of polar residual ice [*Dial*, 1984], remnants of the seasonal CO_2 frost cap [*Thomas et al.*, 1992], and outlying mesas of ice, frost, or polar layered materials [*Tanaka and Scott*, 1987]. Additional polar material remnants have now been identified, and the characteristics of mapped outliers have been better constrained by MOLA data. We propose that the mapped [*Dial*, 1984; *Tanaka and Scott*, 1987] outliers, a subset of the actual total population, are a mix of (1) frost-covered or residual ice-filled craters, (2) frost patches, (3) polar material remnants, consisting mostly of polar layered material, and

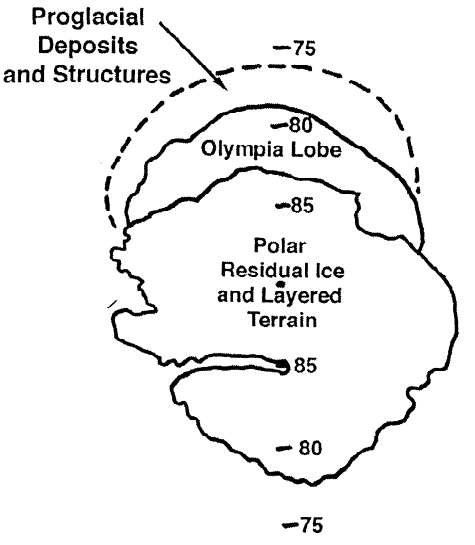

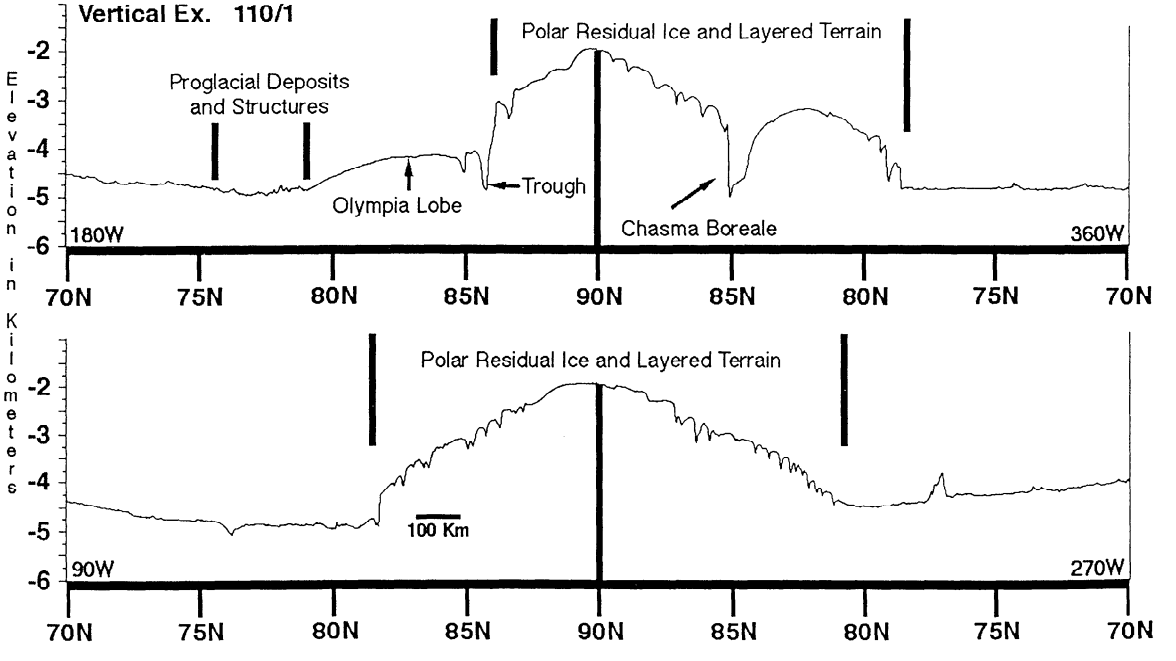

Figure 15. Circumscription of a line at about 77°N around the presently exposed polar deposits and the outlying arc of kettle-like features and polar material remnants, including Olympia Planitia, produces an areal symmetry of the cap about the north rotational pole and suggests that the cap was once larger, extending to this line. We have termed the dune-covered lobe centered at 180°W the Olympia Lobe. Topographic profiles show the relationships of the distal deposits (interpreted to be proglacial deposits and structures), the Olympia Lobe (interpreted to be a large-scale equivalent of an ice-cored moraine), and the main cap (residual ice and layered terrain).

(4) kettles. The following observations support this:

1. Some of the mapped outliers are within a distance of one crater diameter from craters larger than or the same size as the outliers themselves. These outliers thus must represent frost-covered crater topography.

2. Some of the mapped outliers exhibit a flat topography, and thermal inertia data show that thin layers of frost are deposited seasonally and change shape [*Paige et al.*, 1994]. These are thus not polar material remnants.

3. Some of the mapped outliers are within bright patches having no visible craters at 1.75 km resolution, have topographic characteristics which distinguish them from the surrounding terrain and from seasonal frost, and do not change shape significantly from year to year [*Bass et* al., 2000]. Thus these must represent remnants of polar material, probably mostly layered materials as described above.

4. The proposed kettles do not exhibit a regular shape or a depth to diameter ratio similar to fresh craters, exhibit little or no rim topography, and are distinct from the surrounding cratered plains both in topography and roughness [*Kreslavsky and Head*, 1999] maps.

4.3. Implications for the Previous Extent of the Polar Cap

On the basis of the topography of Olympia Planitia and of the mapped Apr outlier arc to the south, we conclude that the

material underlying the longitudinal dunes is an extension of the polar cap deposits and that the arc of outliers and kettle-like features represents remnant morphology of a once larger cap. We have termed this former extension of the cap the Olympia Lobe. Additional evidence to support this conclusion comes from the fact that circumscription of a line surrounding the presently exposed continuous residual ice deposits, Olympia Planitia, and the arc of outliers and kettles produces an areal symmetry around the present rotational pole (Figure 15). *Clifford et al.* [2000] state that the current cap shape is only representative of the current climate so that the polar materials may be interbedded to great distances at depth. In addition, according to the authors, ridges visible beyond the residual cap edge in Viking images between 300° and 360°W represent a former extent of the cap.

The volume of polar material which has been removed from the Olympia Lobe has been calculated by assuming cone shapes delineated by the slopes from the top of the cap to the arc of polar material outliers and to the edge of Olympia Planitia. This minimum estimate yields a volume of $\sim 3 \times 10^5$ km^3. This volume 25% of the current minimum cap volume, estimated to be 1.2×10^6 km^3 by *Zuber et al.* [1998a]. If this estimated volume includes ~40% dust [*Herkenhoff*, 1998], then the amount of dust is equal to ~250x the estimated volume of the north polar ergs (1200 km^3 [*Greeley et al.*, 1992]). Thus ablation of the missing portion of the cap could easily provide enough material for the dunes and part of the surrounding mantle deposits.

Even if the volume estimate of the missing portion of the Olympia Lobe is doubled, the cap volume, including that missing from the Olympia Lobe, is not sufficient to produce basal melting under current conditions (assuming a composition of water ice) according to *Clifford and Parker*'s [2000] hydrological model and *Greve*'s [1998] dynamic/thermodynamic simulations of the cap. However, basal melting could occur during times of high deposition of polar materials or volcanic eruption beneath the cap [*Clifford and Parker*, 2000]. The evidence we have outlined for a formerly larger cap suggests that changes in the polar environment have indeed occurred.

According to *Johnson et al.* [2000], if the circumpolar depression containing the mantled smooth plains is flexural in origin, then the lithosphere is 60 – 120 km thick. This model [*Johnson et al.*, 2000] predicts that for a thin lithosphere (~ 40 km thick) and a polar cap containing a significant fraction of dust, basal melting might be possible. *Johnson et al.* [2000] also state that the presence of dissolved salts at the base would lower the melting temperature. The oceanic and fluvial sediments, inferred to reside beneath the cap according to the current study, could have been a source for these salts. Thus basal melting may have occurred some time in the past beneath the north polar cap. The amount of basal melting also depends on the volatile content of the cap. If the cap is made almost entirely of water ice, then basal melting is not possible under current conditions; *Kargel* [1998] has described this effect using several model compositions. If the cap is made of CO_2 hydrate, then basal melting may occur in places [*Ross and Kargel*, 1998], and the cap may vary about equilibrium. If the cap is made of interlayered CO_2 hydrate and water ice, then basal melting is also possible beneath the cap, the base being at a temperature at or near the melting point. A final possibility would be that the cap is made mostly of CO_2 ice (the least favored model), in which case extensive basal melting could occur. Other support for past basal melting includes the evidence for the occurrence of jökulhlaup-type events which may have carved Chasma Boreale and other similar features within the cap [*Clifford*, 1987; *Benito et al.*, 1997; *Fishbaugh and Head*, 1999, manuscript in preparation, 2000]. An alternative mechanism, erosion by katabatic winds, has been proposed for the origin of the Chasma [*Howard*, 1998], but the deep enclosed depressions, topography of outflow deposits, channel-like features at the mouth, and similar features of different orientations elsewhere within the cap point more toward a jökulhlaup formation.

Tanaka and Leonard [1998] also suggest that the cap may have undergone melting, but the timing is different than the stratigraphy that we are proposing in this study. According to the authors, melting may have occurred during the Hesperian at the same time that the outflow channels were being carved. The authors state that this melting may have been caused by high obliquity or volatile release during the carving of the outflow channels and/or during periods of volcanism.

What factors or processes could have caused retreat of the Olympia Lobe?

1. A decrease in accumulation would move the snow line farther up-cap, thus causing an imbalance in the amount of ablation versus accumulation and a slow retreat by sublimation and wind ablation. Causes for the decrease in accumulation could include variations in H_2O supply due to obliquity cycles [e.g., *Clifford et al., 2000*; *Toon et al.*, 1980] and a decrease in the amount of surface water due to inclusion of ocean and outflow channel water into the cryosphere.

2. An increase in the ablation rates could also cause retreat of the cap. As described above, the eastern half of the outlier arc is rougher than the western half. This asymmetry may be due to preferential deposition of thin layers of pyroclastic ash from Alba Patera in this region. Such ash layers could increase the sublimation rate in this region. Variations in ablation rates could also come from the obliquity cycle [e.g., *Toon et al.*, 1980].

3. Basal melting could also provide a relatively fast mode of release of melted polar materials.

4. Another possible mechanism for creating glacier recession morphology would be the freezing of surface lakes into glaciers, entrainment of debris, and eventual ablation and recession as proposed by *Kargel and Strom* [1992] and *Kargel et al.* [1995] as one explanation for the formation of the thumbprint terrain in the northern plains. According to *Kargel et al.* [1995], deglaciation may have occurred via basal melting, a greenhouse effect, high orbital obliquity, or sublimation, factors which we have considered in this study. Their scenario of formation may not be likely for formation of the north polar cap, because it seems to have formed after the existence of climates suitable to large amounts of surface water and after the formation of outflow channels.

5. *Baker et al.* [1991, 2000] have proposed that a northern ocean, Oceanus Borealis, was episodically formed by outflow channel flooding caused by disruption of the cryosphere by heat from volcanic activity associated with Tharsis. Water from this ocean would form polar caps and be lost to the subsurface and to space. As this water supply was depleted, the formerly expanded polar caps would retreat. Thus, according to this model, the present state of the polar cap may represent the current state of the response of the climate to outflow channel and ocean formation and disappearance.

6. *Fishbaugh and Head* [2000] have pointed out that the directions of retreat of the two polar caps are offset in antipodal directions from each other. Polar wander [*Schultz and Lutz*,

1988] is one possible mechanism that could accomplish this configuration.

The current dynamic state of the cap is not clear, that is, whether it is currently in a state of net erosion or in a steady-state condition [*Howard et al.*, 1982; *Fisher*, 1993; *Muhleman and Ivanov*, 1998; *Zuber et al.*, 1998b; *Clifford et al.*, 2000]. Because low obliquity causes reduction in dust storm activity, and high obliquity causes increased sublimation, significant accumulation may be able to take place only during times of moderate obliquity (i.e., the current climate) if condensation of dust particles is the major means of deposition on the poles [*Clifford et al., 2000*]. However, the accumulation rate seems to be decreasing, as evidenced by the fact that images of the cap from different seasons expose the same layers even after the winter deposition of frost has receded. In addition, *Bass et al.* [2000] suggest that accumulation is currently taking place near the center of the cap. *Clifford et al.* [2000] describe the cap as accumulating in the center and having a pattern of spiraling ablation and accumulation in the form of troughs. According to the authors, ablation of the cap has a greater influence in the present dynamics than does glacier flow, as is evidenced by the existence of the troughs.

Fisher [1993] has described an "accublation" model of cap dynamics. According to this model, most of the ablation of the cap may be occurring within the troughs. Spiral troughs form at places where the migration velocity of the scarps toward the center of the cap and down and outward flow velocity of the ice are equal. Ablation occurs on the south facing walls of these troughs. This ablation would leave sediment as a lag deposit, some of which would be redistributed by the wind and some of which would end up moving downward so that trough migration leaves a layer of sediment at the base of the cap, an analog to a moraine. Evidence of these basal "moraine" layers in images might provide further information about the former cap edge.

The presence of a thick eolian mantling on the polar materials of Olympia Planitia would imply that sublimation or wind ablation does not affect these polar deposits. Sublimation and wind ablation are probably the main mechanisms of ablation at this time, with different parts of the cap eroding at different rates. *Muhleman and Ivanov* [1998] propose that the current shape of the polar cap is due to ablation. *Zuber et al.* [1998b] find that, using a power law flow model in which accumulation balances ablation from the edges, and assuming a cylindrical ice sheet, the northern cap fits very small accumulation rates best. They interpret this to imply that the cap is not moving or is getting smaller (not including seasonal changes).

Further studies will include detailed examination of the kettle-like topography and morphology, investigation into possible modes of asymmetrical cap retreat with comparison to similar terrestrial processes, and examination of evidence, using MOLA and Viking/MOC images, for basal melting and cap flow. We have begun preliminary comparisons between the geological histories of the two Martian polar regions, and evidence has been found for retreat of Hesperian polar-like deposits in the south [*Head*, 2000a, 2000b].

Acknowledgments. We gratefully acknowledge the MOLA instrument team and the MGS spacecraft and operations teams at the Jet Propulsion Laboratory and Lockheed-Martin Astronautics for providing the engineering foundation that enabled this analysis. We particularly thank Greg Neumann and Steve Pratt for superior professional performance in data reduction and preparation. Jeff Kargel and Ken Tanaka provided very helpful reviews of this paper.

References

Ahronson, O., M. Zuber., G. Neumann, and J. Head, Mars: Northern hemisphere slopes and slope distribution, *Geophys. Res. Lett., 25*, 4413-4416, 1998.

Anguita, F., R. Babin, G. Benito, A. Collado, D. Gomez, and J. Rice, Chasma Australe, Mars: Structural framework for a catastrophic outflow origin, in *1st International Conference on Mars Polar Science and Exploration, LPI Contrib. 953*, p. 1, Lunar and Planet. Inst., Camp Allen, Tex., 1998.

Anguita, F., R. Babin, G. Benito, D. Gomez, A. Collado, and J. Rice, Chasma Australe, Mars: Structural framework for a catastrophic outflow origin, *Icarus*, *144*, 302-312, 2000.

Baker, V., R. Strom, V. Gulick, J. Kargel, G. Komatsu, and V. Kale, Ancient oceans, ice sheets and the hydrological cycle on Mars, *Nature*, *352*, 589-594, 1991.

Baker, V., M. Carr, V. Gulick, C. Williams, and M. Marley, Channels and valley networks, in *Mars*, edited by H. Kieffer et al., pp. 493-522, Univ. of Ariz. Press, Tucson, 1992.

Baker, V., R. Strom, J. Dohm, V. Gulick, J. Kargel, G. Komatsu, G. Ori, and J. Rice, Mars: Oceanus Borealis, ancient glaciers, and the MEGAOUTFLO hypothesis, *Lunar Planet. Sci.* [CD-ROM] *XXXI*, abstract 1836, Lunar Planet. Sci. Inst., Houston, Tex., 2000.

Banin, A., B. Clark, and H. Wänke, Surface chemistry and mineralogy, in *Mars*, edited by H. Kieffer et al., pp. 594-625, Univ. of Ariz. Press, Tucson, 1992

Bass, D., K. Herkenhoff, and D. Paige, Variability of Mars' north polar water ice cap, I: Analysis of Mariner 9 and Viking Orbiter imaging data, *Icarus*, *144*, 382-396.

Benito, G., F. Mediavilla, M. Fernandez, A. Marquez, J. Martinez, and F. Anguita, Chasma Boreale: A sapping and outflow channel with a tectono-thermal origin, *Icarus*, *129*, 528-538, 1997.

Benn, D., and D. Evans, *Glaciers and Glaciation*, pp. 244 and 492-493, Cambridge University Press, New York, 1998.

Breed, C., M. Grolier, and J. McCauley, Morphology and distribution of common sand dunes on Mars: Comparison with Earth, *J. Geophys. Res.*, *84*, 8183-8204, 1979.

Cantor, B., M. Wolff, P. James, and E. Higgs, Regression of Martian north polar cap: 1990-1997 Hubble Space Telescope observations, *Icarus*, *136*, 175-191, 1998.

Carr, M., *Water on Mars*, pp. 493–522, Oxford Univ. Press, New York, 1996.

Clark, R., Kettle holes, *J. Glaciol.*, *54*, 485-486, 1969.

Clifford, S., Polar basal melting on Mars, *J. Geophys. Res.*, *92*, 9135-9152, 1987.

Clifford, S., A model for the hydrologic and climatic behavior of water on Mars, *J. Geophys. Res.*, *98*, 10,973-11,016, 1993.

Clifford, S., and T. Parker, Hydraulic and thermal arguments regarding the existence and fate of a primordial Martian ocean, *Lunar Planet. Sci.* , [CD-ROM] *XXX*, abstract 1619, Lunar Planet. Sci. Inst., Houston, Tex., 1999.

Clifford, S., et al., The state and future of Mars polar science and exploration, *Icarus*, *144*, 210-242, 2000.

Clifford, S., and T. Parker, The evolution of the Martian hydrosphere and implications for the fate of a primordial ocean and the current state of the northern plains, *Icarus*, in press, 2000.

Costard, F., and J. Kargel, Outwash plains and thermokarst on Mars, *Icarus*, *114*, 93-112, 1995.

Cutts, J., K. Blasius, G. Briggs, M. Carr, R. Greeley, and H. Masursky, North polar region of Mars: Imaging results from Viking 2, *Science*, *194*, 1329-1337, 1976.

Desloges, J., and M. Church, Geomorphic implications of glacier outburst flooding: Noeick River valley, British Columbia, *Can. J. Earth Sci.*, *29*, 551-564, 1992.

Dial, A., Geologic map of the Mare Boreum region of Mars, *U.S. Geol. Surv. Misc. Invest. Map, I-1640*, 1984.

Dial, A., and J. Dohm, Geologic map of science study area 4, Chasma Boreale region of Mars, *U.S. Geol. Surv. Misc. Invest. Map, I-2357*, 1994.

Fishbaugh, K., and J. Head, The geometry of Chasma Boreale, Mars using Mars Orbiter Laser Altimeter (MOLA) data: A test of the catastrophic outflow hypothesis of formation, in *5th International Conference on Mars* [CD-ROM], abstract 6187, Lunar and Planet. Inst., Pasadena, Calif., 1999.

Fishbaugh, K., and J. Head, Comparison of the north and south polar caps of Mars: New insights from MOLA data, *Lunar Planet. Sci.* [CD-

ROM] XXXI, abstract 1637, Lunar Planet. Sci. Inst., Houston, Tex., 2000.

Fisher, D., If Martian ice caps flow: Ablation mechanisms and appearance, *Icarus*, *105*, 501-511, 1993.

Flint, R., *Glacial and Pleistocene Geology*, pp. 71, 140, 149, 151, 152, John Wiley, New York, 1963.

Forget, F., Formation of the carbon dioxide ice seasonal polar caps, in *1st International Conference on Mars Polar Science and Exploration, LPI Contrib. 953*, p. 11, Lunar and Planet. Inst., Camp Allen, Tex., 1998.

Garvin, J., and J. Frawley, Geometric properties of Martian impact craters: Preliminary results from the Mars Orbiter Laser Altimeter, *Geophys. Res. Lett.*, *25*, 4405 -4408, 1998.

Garvin, J., S. Sakimoto, J. Frawley, and A. Matias, Martian north polar region impact craters: Geometric properties from Mars Orbiter Laser Altimeter (MOLA) observations, in *1st International Conference on Mars Polar Science and Exploration, LPI Contrib. 953*, pp. 12-13, Lunar and Planet. Inst., Camp Allen, Tex., 1998.

Garvin, J., S. Sakimoto, J. Frawley, and C. Schnetzler, North polar region craterforms on Mars: Geometric characteristics from the Mars Orbiter Laser Altimeter, *Icarus*, *144*, 329-252, 2000.

Greeley, R., N. Lancaster, S. Lee, and P. Thomas, Martian eolian processes, sediments, and features, in *Mars*, edited by H. H. Kieffer et al., pp. 730-766, Univ. of Ariz. Press, Tucson, 1992.

Greve, R., Dynamic/thermodynamic simulations of the north polar ice cap of Mars, in *1st International Conference on Mars Polar Science and Exploration, LPI Contrib. 953*, pp. 13-15, Lunar and Planet. Inst., Camp Allen, Tex., 1998.

Gulick, V., and V. Baker, Fluvial valleys and Martian paleoclimates, *Nature*, *341*, 514-516, 1989.

Head, J., Extensive south polar ice cap in Middle Mars history?: tests using MOLA data, *Lunar Planet. Sci.* [CD-ROM] *XXXI*, abstract 1119, Lunar Planet. Sci. Inst., Houston, Tex., 2000a.

Head, J., Mars south pole: Evidence for geologically recent lateral migration of volatile-rich layered deposits, *Lunar Planet. Sci.* [CD-ROM] *XXXI*, abstract 2036, Lunar Planet. Sci. Inst., Houston, Tex., 2000b.

Head, J., M. Kreslavsky, H. Hiesinger, M. Ivanov, S. Pratt, N. Seibert, D. Smith, and M. Zuber, Oceans in the past history of Mars: Tests for their presence using Mars Orbiter Laser Altimeter (MOLA) data, *Geophys. Res. Lett.*, *25*, 4401-4404, 1998.

Head, J., M. Kreslavsky, H. Hiesinger, and S. Pratt, Northern seas and oceans in the past history of Mars: New evidence from Mars Orbiter Laser Altimeter (MOLA) data, *Lunar Planet. Sci.* [CD-ROM] *XXX*, abstract 1352, Lunar Planet. Sci. Inst., Houston, Tex., 1999a.

Head, J., H. Hiesinger, M. Ivanov, M. Kreslavsky, S. Pratt, and B. Thomson, Possible ancient oceans on Mars: Evidence from Mars Orbiter Laser Altimeter data, *Science*, *286*, 2134-2137, 1999b.

Herkenhoff, K., Geology, composition, age, and stratigraphy of the polar layered deposits on Mars, *1st International Conference on Mars Polar Science and Exploration, LPI Contrib. 953*, pp. 18-19, Lunar and Planet. Inst., Camp Allen, Tex., 1998.

Herkenhoff, K., and J. Plaut, Surface ages and resurfacing rates of the polar layered deposits on Mars, *Icarus*, *144*, 243-255, 2000.

Herkenhoff, K., J. Plaut, and S. Nowicki, Surface age and resurfacing rate of the north polar layered terrain on Mars, *Proc. Lunar Planet. Sci. Conf. 28th*, pp. 551-552, Lunar Planet. Sci. Inst., Houston, Tex., 1997.

Hiesinger, H., and J. Head, Polygonal terrain of Utopia Planitia, Mars: The first MOLA results, *Lunar Planet. Sci.* [CD-ROM] *XXX*, abstract 1354, Lunar Planet. Sci. Inst., Houston, Tex., 1999.

Hiesinger, H., and J. Head, Characteristics and origin of polygonal terrain in southern Utopia Planitia, Mars: Preliminary results from Mars Orbiter Laser Altimeter (MOLA) and Mars Orbiter Camera (MOC) data, *J. Geophys. Res.*, *105*, 11,999-12,022, 2000.

Howard, A., The role of eolian processes in forming Martian polar topography, *1st International Conference on Mars Polar Science and Exploration, LPI Contrib. 953*, pp. 19-21, Lunar and Planet. Inst., Camp Allen, Tex., 1998.

Howard, A., J. Cutts, and K. Blasius, Stratigraphic relationships within Martian polar cap deposits, *Icarus*, *50*, 161-215, 1982.

Ivanov, M., and J. Head, Chryse Planitia, Mars: Topographic configuration from MOLA data and tests for hypothesized lakes and shorelines, *5th International Conference on Mars* [CD-ROM], abstract 6176, Lunar Planet. Sci. Inst., Pasadena, Calif., 1999.

Jager, K., and J. Head, Alba Patera, Mars: Characterization using Mars Orbiter Laser Altimeter (MOLA) data and comparison with other volcanic edifices, *Lunar Planet. Sci.* [CD-ROM] *XXX*, abstract 1915, Lunar and Planet. Inst., Houston, Tex., 1999.

Johnson, C., S. Solomon, J. Head, R. Phillips, D. Smith, and M. Zuber, Lithospheric loading by the northern polar cap on Mars, *Icarus*, *144*, 313-328, 2000.

Kargel, J., Possible composition of the Martian polar caps and controls on ice cap behavior, in *1st International Conference on Mars Polar Science and Exploration, LPI Contrib. 953*, pp. 22-23, Lunar and Planet. Inst., Camp Allen, Tex., 1998.

Kargel, J., and R. Strom, Ancient glaciation on Mars, *Geology*, *20*, 3-7, 1992.

Kargel, J., V. Baker, J. Beget, J. Lockwood, T. Pewe, J. Shaw, and R. Strom, Evidence of ancient continental glaciation in the Martian northern plains, *J. Geophys. Res.*, *100* (E3), 5351-5368, 1995.

Khan, R., T. Martin, and R. Zurek, The Martian dust cycle, in *Mars*, edited by H. H. Kieffer et al., pp. 1017-1053, Univ. Ariz. Press, Tucson, 1992.

Kieffer, H., S. Chase, T. Martin, E. Miner, and F. Palluconi, Martian north pole summer temperature: Dirty water-ice, *Science*, *194*, 1342-1344, 1976.

Kieffer, H., T. Martin, A. Peterfreund, and B. Jakosky, Thermal and albedo mapping of Mars during the Viking primary mission, *J. Geophys. Res.*, *82*, 4249-4291, 1977.

Kreslavsky, M., and J. Head, Kilometer-scale slopes on Mars and their correlation with geologic units: Initial results from Mars Orbiter Laser Altimeter (MOLA) data, *J. Geophys. Res.*, *104*, 21,911-21,924, 1999.

Lucchitta, B., H. Ferguson, and C. Summers, Sedimentary deposits in the northern lowland plains, Mars, *Proc. Lunar and Planet. Sci. Conf. 17th*, Part 1, *J. Geophys. Res.*, *91*, suppl., E166-E174, 1986.

Muhleman, D., and A. Ivanov, Evolution of the Mars northern ice cap and results from Mars Observer Laser Altimeter (MOLA), in *1st International Conference on Mars Polar Science and Exploration, LPI Contrib. 953*, pp. 28-29, Lunar and Planet. Inst., Camp Allen, Tex., 1998.

Paige, D., J. Bachman, and K. Keegan, Thermal and albedo mapping of the polar regions of Mars using Viking Thermal Mapper observations, 1. North polar region, *J. Geophys. Res.*, *99*, 25,959-25,991, 1994.

Parker, T., R. Saunders, and D. Schneeberger, Transitional morphology in West Deuteronilus Mensae, Mars: Implications for modification of the lowland/highland boundary, *Icarus*, *76*, 357-377, 1989.

Parker, T., D. Gorsline, R. Saunders, D. Pieri, and D. Schneeberger, Coastal geomorphology of the Martian northern plains, *J. Geophys. Res.*, *98*, 11,061-11,078, 1993.

Plaut, J., R. Kahn, E. Guiness, and R. Arvidson, Accumulation of sedimentary debris in the south polar region of Mars and implications for climate history, *Icarus*, *76*, 357-377, 1988.

Ross, R., and J. Kargel, Thermal conductivity of solar system ices with special reference to Martian polar caps, in *Solar System Ices*, edited by B. Schmitt et al., pp. 33-62, Kluwer Acad., Norwell, Mass., 1998.

Schultz, P., and A. Lutz, Polar wandering of Mars, *Icarus*, *73*, 91-141, 1988.

Scott, D., J. Dohm, and J. Rice, Map of Mars showing channels and possible paleolake basins, *U.S. Geol. Surv. Misc. Invest. Ser. Map, I-2461*, 1995.

Smith, D., et al., Topography of the northern hemisphere of Mars from the Mars Orbiter Laser Altimeter, *Science*, *279*, 1686-1692, 1998.

Smith, D., et al., The global topography of Mars and implications for surface evolution, *Science*, *284*, 1495-1503, 1999.

Soderblom, L., T. Kriedler, and M. Harold, Latitudinal distribution of a debris mantle on the Martian surface, *J. Geophys. Res.*, *78*, 4117-4122, 1973a.

Soderblom, L., M. Malin, J. Cutts, and B. Murray, Mariner 9 observations of the surface of mars in the North Polar Region, *J. Geophys. Res.*, *78*, 4197-4210, 1973b.

Squyres, S., The evolution of dust deposits in the Martian north polar region, *Icarus*, *40*, 244-261, 1979.

Tanaka, K., and G. Leonard, Martian paleopolar deposits: Evidence for a stable pole and periods of climate change, in *1st International Conference on Mars Polar Science and Exploration, LPI Contrib. 953*, pp. 39-40, Lunar and Planet. Inst., Camp Allen, Tex., 1998.

Tanaka, K., and D. Scott, Geologic map of the polar regions of Mars, *U.S. Geol. Surv. Misc. Invest. Ser. Map, I-1802-C*, 1987.

Tanaka, K., D. Scott, and R. Greeley, Global stratigraphy, in *Mars*, edited by H. H. Kieffer et al., pp. 345-382, Univ. of Ariz. Press, Tucson, 1992.

Thomas, P., and C. Weitz, Sand dune materials and polar layered deposits on Mars, *Icarus*, *81*, 185-215, 1989.

Thomas, P., S. Squyres, K. Herkenhoff, A. Howard, and B. Murray, Polar deposits of Mars, in *Mars*, edited by H. H. Kieffer et al., pp. 767-795, Univ. of Ariz. Press, Tucson, 1992.

Thomson, B., and J. Head, Utopia Basin, Mars: A new assessment using Mars Orbiter Laser Altimeter (MOLA) data, *Lunar Planet. Sci.* [CD-ROM] *XXX*, abstract 1894, Lunar and Planet. Inst., Houston, Tex., 1999.

Toon, O., J. Pollack, W. Ward, J. Burns, and K. Bilski, The astronomical theory of climate change on Mars, *Icarus*, *44*, 552-607, 1980.

United States Geological Survey (USGS), Topographic maps of the Polar, Western, and Eastern regions of Mars, *U.S. Geol. Surv. Misc. Invest. Series Map, I-2160,* 1991.

Zuber, M., et al., Observations of the North Polar region of Mars from the Mars Orbiter Laser Altimeter, *Science*, *282*, 2053-2060, 1998a.

Zuber, M., L. Lim, and H. Zwally, The role of viscous deformation in the morphology of the Martian north polar cap, 1st International Conference on Mars Polar Science, *LPI Contrib. 953*, pp. 435-436, Lunar and Planet. Inst., Houston, Tex., 1998b.

K. E. Fishbaugh and J. W. Head III, Department of Geological Sciences, Brown University, Box 1846, Providence, RI 02912. (kathryn_fishbaugh@brown.edu; james_head_III@brown.edu)

(Received December 19, 1999; revised May 5, 2000; accepted May 16, 2000.)